ON SELF-INTERFERENCE CANCELLATION IN WIRELESS FULL DUPLEX

A THESIS SUBMITTED TO
THE GRADUATE SCHOOL OF NATURAL AND APPLIED SCIENCES
OF
MIDDLE EAST TECHNICAL UNIVERSITY

BY

AKSAY FATIH ÖNCEL

IN PARTIAL FULFILLMENT OF THE REQUIREMENTS
FOR
THE DEGREE OF MASTER OF SCIENCE
IN
ELECTRICAL AND ELECTRONICS ENGINEERING

AUGUST 2016

Approval of the thesis:

ON SELF-INTERFERENCE CANCELLATION IN WIRELESS FULL DUPLEX

submitted by **AKSAY FATIH ÖNCEL** in partial fulfillment of the requirements for the degree of **Master of Science in Electrical and Electronics Engineering Department, Middle East Technical University** by,

Prof. Dr. Gülbin Dural Ünver
Dean, Graduate School of **Natural and Applied Sciences** _____

Prof. Dr. Tolga Çiloğlu
Head of Department, **Electrical and Electronics Engineering** _____

Prof. Dr. Ali Özgür Yılmaz
Supervisor, **Electrical and Electronics Engineering Department, METU** _____

Assist. Prof. Dr. Fatih Koçer
Co-supervisor, **Electrical and Electronics Engineering Department, METU** _____

Examining Committee Members:

Prof. Dr. Elif Uysal Bıyıkoğlu
Electrical and Electronics Engineering Department, METU _____

Prof. Dr. Ali Özgür Yılmaz
Electrical and Electronics Engineering Department, METU _____

Assist. Prof. Dr. Fatih Koçer
Electrical and Electronics Engineering Department, METU _____

Prof. Dr. Sencer Koç
Electrical and Electronics Engineering Department, METU _____

Assoc. Prof. Dr. Cenk Toker
Electrical and Electronics Eng. Dep., Hacettepe University _____

Date: _____

I hereby declare that all information in this document has been obtained and presented in accordance with academic rules and ethical conduct. I also declare that, as required by these rules and conduct, I have fully cited and referenced all material and results that are not original to this work.

Name, Last Name: AKSAY FATIH ÖNCEL

Signature :

ABSTRACT

ON SELF-INTERFERENCE CANCELLATION IN WIRELESS FULL DUPLEX

Öncel, Aksay Fatih
M.S., Department of Electrical and Electronics Engineering
Supervisor : Prof. Dr. Ali Özgür Yılmaz
Co-Supervisor : Assist. Prof. Dr. Fatih Koçer

August 2016, 79 pages

Full duplex is a newly promising duplexing method. Unlike traditional time division or frequency division duplexing, in full duplex the transmit and receive signals of a transceiver are active at the same time and in the same frequency band. This can double the spectral efficiency. However, since the transmit signal is typically much more powerful than the receive signal at the receive antenna, it acts as a strong interferer to the received signal and this interference must be mitigated first, in order to fully leverage full duplex.

Until recently, because of the interference problem, the use of full duplex in data communications was generally avoided. Recently, however, as a result of demand for higher spectral efficiency especially for future generation cellular and wireless communications, research advances are made in the mitigation of this interference which paved the way for achieving practical full duplex.

In this thesis the following work has been done, 1) a survey of full duplex with its brief history and recent advances is presented, 2) critical presentation and analysis of selected methods of self-interference cancellation in analog and digital domains are made, 3) a selected adaptive filtering method is expanded, 4) selected methods' and expansion's performance are evaluated with simulations, 5) experiments are carried out using software defined radios.

It was shown with experiments and simulations that, local oscillator phase noise constitutes a bottleneck for full duplex operation. In simulations, without phase noise, cancellation of self-interference up to the thermal noise floor is accomplished. However, in the presence of phase noise in experiments, also verified by simulations, the cancellation in digital domain hits a limit which prevents complete cancellation of self-interference after a certain power. This limitation impels the use of other means of self interference cancellation than digital, if one wishes to cancel out all self interference even at high powers.

Keywords: full duplex radio, self-interference, digital cancellation, analog cancellation

ÖZ

KABLOSUZ FULL DUPLEKSTE ÖZ-GİRİŞİM BASTIRMA ÜZERİNE

Öncel, Aksay Fatih
Yüksek Lisans, Elektrik ve Elektronik Mühendisliği Bölümü
Tez Yöneticisi : Prof. Dr. Ali Özgür Yılmaz
Ortak Tez Yöneticisi : Yrd. Doç. Dr. Fatih Koçer

Ağustos 2016 , 79 sayfa

Tam çoklama (full duplex), kablosuz haberleşmede ümid vaad eden yeni bir çoklama tekniğidir. Geleneksel zaman veya frekans bölümlü çoklamaların aksine, tam çoklama yapan bir alıcı-vericide, alınan ve verilen sinyaller aynı anda ve aynı frekans bandında aktiftirler. Bu eş kullanım spektrum verimliliğini iki misline çıkarabilir. Fakat, bir alıcı-vericinin kendi gönderdiği sinyal, onun alıcısında karşıdan gelen sinyale göre çok daha kuvvetli görülmektedir. Bu sebeple, radyonun kendi gönderdiği sinyal karşıdan aldığı sinyale çok kuvvetli bir girişim olarak tesir eder. Tam çoklamadan tam istifade edebilmek için bu girişimin bir şekilde bastırılması gerekir.

Girişim sorunu yüzünden yakın zamana dek kablosuz veri haberleşmesinde tam çoklamadan kaçınılmıştır. Yakın zamanda özellikle ileri nesil hücresel ve kablosuz haberleşmedeki yüksek spektrum verimliliği talepleri üzerine girişim bastırma araştırmaları yoğunlaşmış ve pratik tam çoklamanın önü açılmıştır.

Bu tezde sıradaki çalışmalar yapılmıştır: 1) tam çoklama, kısa bir tarihçesi ve yakın zamandaki gelişmeleriyle etüt edilmiş, 2) seçilen bazı analog ve dijital bastırma yöntemleri analiz edilmiş ve eleştirel sunumları yapılmış, 3) seçilen bir uyarlamalı süzgeç yöntemi genişletilmiş, 4) seçilen ve genişletilmiş metotların performansları benzetimlerle (simülasyon) ölçülmüş, 5) *software defined* radyolar kullanılarak deneyler yapılmıştır.

Benzetim ve deneylerle gösterilmiştir ki yerel salınıcı faz gürültüsü tam çoklama için bir darboğaz oluşturmaktadır. Faz gürültüsüz benzetimlerde girişim termal gürültü tabanına kadar bastırılabilmiştir. Faz gürültüsünün mevcut olduğu deneylerde, ve benzetimlerle teyid edildiği üzere, dijital bastırma belirli bir seviyede sabit kalmış ve belirli bir seviyenin üstündeki girişim güçleri için tam bastırma sağlanamamıştır. Dijital bastırmadaki bu sınır, termal gürültü tabanına kadar girişim bastırma hedefi için dijital bastırma harici yöntemleri (örn. analog) zorunlu kılmaktadır.

Anahtar Kelimeler: full duplex radyo, öz-girişim, dijital bastırma, analog bastırma

ACKNOWLEDGMENTS

I would like to acknowledge TÜBİTAK for providing me with the grant "TÜBİTAK 2211 Yurt İçi Lisansüstü Burs Programı" during my thesis studies.

I send my sincere gratitude to my family and friends, who all helped me someway during my master's studies.

I wish to acknowledge and thank for the great help of my advisor Ali Özgür Yılmaz and co-advisor Fatih Koçer. If it were not for them, this thesis would not be in its current state now. I express my best regards to my peer Ufuk Tamer, who helped me with the experimental measurements and else.

TABLE OF CONTENTS

LIST OF TABLES

TABLES

LIST OF FIGURES

FIGURES

LIST OF ALGORITHMS

ALGORITHMS

LIST OF ABBREVIATIONS

IBFD	In-band full duplex
SI	Self-interference
SIC	Self-interference Cancellation
SNR	Signal-to-noise ratio
SINR	Signal-to-interference-plus-noise ratio
PA	Power amplifier
EVM	Error Vector Magnitude

CHAPTER 1

INTRODUCTION

Wireless communications technology is in constant progress since its emergence. However, it is especially the last few decades that saw a rocketing increase in demand for higher data rates and lower latencies in contemporary consumer applications, e.g., Wi-Fi and cellular (4G, 5G). To meet this demand, evolutionary technologies for 5G are expected to be implemented in the near future [1, 2, 3, 4]. Additionally, Third Generation Partnership Project (3GPP) has issued a roadmap for 5G [5], wherein high spectral efficiency, among other things, is proposed to increase the wireless capacity. This has led the researchers' attention to increasing the spectral efficiency. One of the most promising enablers of this high efficiency is the in-band full-duplex (IBFD) communications.

IBFD can be defined as a communication method, where the transmission and reception on a transceiver take place simultaneously and in the same frequency band. Traditionally, the half-duplex and out-of-band full-duplex refer to the time division and frequency division duplexing, respectively. Time division duplexing (half duplex) uses orthogonal time slots for transmission and reception. Likewise, frequency division duplexing (out-of-band full duplex) uses orthogonal frequency slots for transmission and reception. In IBFD, however, there is no orthogonality between the transmission and reception. Consequently, there is a strong self-interference (SI), viz., the coupling of one's transmission to its own reception. The frequency band designation (in-band vs. out-of-band) is made in order to differentiate this new technology, IBFD, from the traditional frequency division duplexing. Because full-duplex, alone, conventionally means any way of simultaneous transmission and reception. In IBFD literature, and

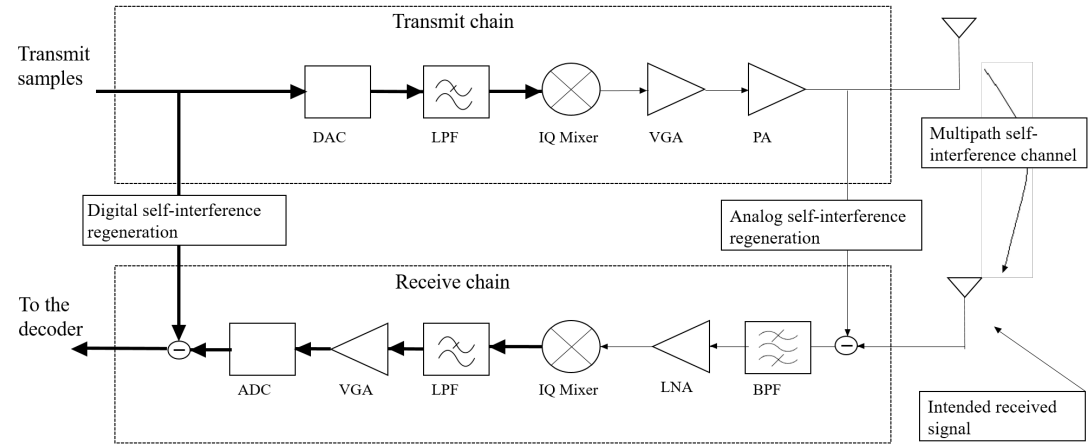

Figure 1.1: IBFD transceiver with separate antenna configuration

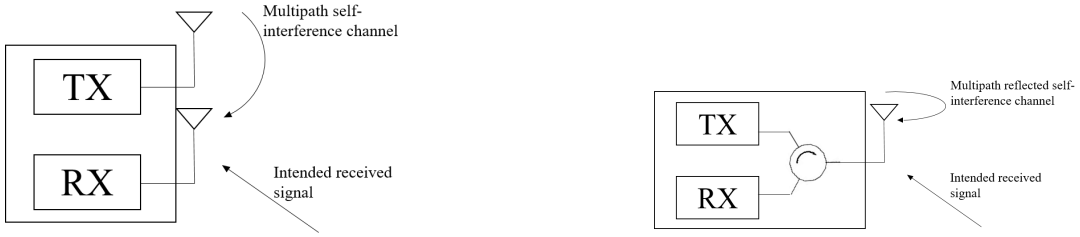

(a) Separate antenna (b) Shared antenna

Figure 1.2: Different antenna configurations for IBFD

also in this thesis, if otherwise is not explicitly stated, *full duplex* exclusively means the *in-band full duplex*.

In Figure 1.1, an IBFD transceiver with separate antennas for transmission and reception can be seen. The transmit signal of the transceiver acts as a strong interferer to the reception because of the close proximity of two antennas. Suppression of this cancellation is employed in digital and analog domains as shown in relevant stages of the transceiver paths. There can also be a shared antenna configuration, which is shown along the separate antenna configuration in Figure 1.2. The shared antenna configuration employs, typically, an isolator to achieve some self interference suppression before SI enters the receive path.

Some advantages of IBFD, which will be later discussed in detail in Section 2.2, can be listed here as:

- Double the spectral efficiency, as measured by the bits communicated successfully per second per Hertz. The usage of the same frequency and time resources by both transmission and reception can double the spectral efficiency hence the link capacity.

- Improved feedback capabilities: to be able to receive feedback, e.g., channel state information (CSI), acknowledgement/negative-acknowledgement, etc., about the ongoing transmission before that transmission ends, gives the transmitter better adaptivity and adjustment capability, [120].

- Increased network secrecy: e.g. in a two node IBFD scenario where both nodes transmit simultaneously, the mixed signal will be challenging for any eavesdropper to discern and decode [6, 7, 8].

- Improved relaying: unidirectional communications (relaying) will benefit by a lower latency, because the relay does not have to wait for the reception to end to begin relaying (transmitting), and vice versa [9, 10].

- Spectrum use flexibility: the same frequency band can be used for different purposes simultaneously: as in a cellular scenario, where downlink and uplink (or backhaul) are traditionally out-of-band full-duplex can be made IBFD, thus save up on the expensive commercial spectrum [11, 12, 13, 14].

The main reason that prevented the common use of the IBFD so far, despite the appealing opportunities listed above, is the self-interference, [15]. In practical IBFD systems, a node's transmit and receive antenna are located very close so that the isolation between them is very small compared to the path loss experienced by the incoming signal (intended received signal sent by other nodes), as a result the received SI is much stronger than the incoming intended received signal at the receive antenna. A numerical example can put this phenomenon in numbers: from [16], a mobile user equipment can transmit at 21 dBm with receiver noise floor at -100 dBm. Assuming a natural spatial isolation (i.e. free space path loss) of 20 dB between a node's transmit and receive antennas, the self-interference signal will be 21-20-(-100)=101 dB above the noise floor. So, if one wishes to eliminate self-interference to the noise floor (cancellation of the SI beyond the noise floor is possible but not necessary [92])

and communicate interference-free as in an ideal non-IBFD system, 101 dB reduction in the SI must be accomplished. Even in the case that some moderate residual self-interference is tolerated; path loss seen by a node at the edge of a small-cell can be around 100 dB, which translates to a received signal power of 21-100=-79 dBm. Adding the 5 dB signal-to-noise ratio (SNR) margin for reliable communications for IEEE 802.11 WLAN, [139], 21-20-(-79-5)=85 dB of reduction is needed in SI signal power.

Impediments to practical IBFDs can be summarized as:

- Self-Interference: as discussed above, the SI will cause the signal-to-interference-plus-noise ratio (SINR), here the interference is attributed primarily to SI, of the intended received signal to be extremely low (several tens of minus dB), therefore disabling any kind of decoding of the intended received signal.
- Inter-user interference: although not as severe as self-interference, the inter-user interference can cause performance degradation as well, because the neighbouring nodes, as they also use the same time and frequency resources, will increase the aggregated interference.
- Self-interference reduction cost: reducing the SI will demand a considerable amount of system resources and energy. A cost-benefit analysis of implementing this system may not always be in favor of IBFD.

The self-interference must be dealt with in order to fully benefit from IBFD. In recent years, there is a growing interest in this subject matter (see Section 2.1.2). The common name given to the self-interference reduction is self-interference cancellation (SIC) in the literature and also in this thesis. This cancellation can be done in following domains: 1) propagation domain, 2) analog domain, and 3) digital domain.

The propagation domain efforts are concentrated on mitigating the SI as much as possible before it reaches one's own receive antenna. This can be accomplished by distant antenna placement, cross polarization, beamforming and antenna directionality. These techniques, however, may have altering effects on intended transmission as well, thus these SIC methods should be designed taking into account the transmitted signal's reception by the other nodes as well.

After the reception of the mixed signal (SI plus intended received signal), analog domain cancellation comes next. Although cancelling in digital domain is more effective, the still-high level of SI can alter the rest of the cancellation performance if it is not mitigated somehow before reaching the analog-to-digital converter (ADC). A reason for analog domain cancellation necessity is the limited dynamic range of ADC devices. This dynamic range creates a bottleneck for the whole cancellation, because the amount of digital cancellation can be at most equal to the dynamic range of the ADC. To put this phenomenon in numbers, let us assume an ADC with 12 bits resolution [17], which will yield an effective number of bits (ENOB) fewer than 12 bits depending on the application, [18, 19]. Optimistically let us assume the ENOB is only 1 bit fewer and equal to 11 bits. The rule of thumb for calculating the dynamic range is 6.02*ENOB dB, [140]. Then, even ignoring the clipping margin of 6 dB (1 bit), and another 6 dB (1 bit) reserved for placing the quantization floor 6 dB under the noise floor in order not to make the system quantization limited, 6.02*11=66.22 dB is the dynamic range. This means that the digital cancellation, even if it is done perfectly, can only cancel 66.22 dB; borrowing from above, 21-20-66.22-(-100)=34.78 dB of residual SI is still left above noise floor and there is no way left to cancel it. Another reason for employing analog cancellation is to reduce the power of the received signal as much as possible before entering the receiver power amplifier (i.e. low noise amplifier (LNA)) in order not to drive the LNA into the nonlinear region or saturation.

Analog domain cancellation is typically done by tapping the transmitted signal (SI) before the transmit antenna, then proccessing it to best match it to the received SI and subtracting it from the total received signal after the receive antenna. This processing, basically, tries to mimic the channel response as seen by the self-interference signal from where it is tapped to where the subtraction takes place. Although some stages of it can be done digitally, the subtraction must be made in analog domain before the received signal reaches ADC.

Digital domain cancellation uses tapped transmit SI signal in digital baseband by processing it to best match it to the received SI and cancels the SI in digital domain. The implementation of digital cancellation is much easier and efficient than analog because it relies on the readily mature and efficient digital signal processing techniques.

In this thesis, selected SIC methods in analog and digital domain proposed recently in the literature are studied. Their detailed analysis is made and their results are verified with simulations and experiments. Some comments on them are made and some extensions to them are derived. Our analyses, complemented with measurement results, show that local oscillator phase noise is the bottleneck for practical IBFD.

1.1 Thesis Outline

The rest of this thesis is organized as follows. In Chapter 2, a comprehensive survey of IBFD is presented. Its brief history in radars and data communications are presented, and recent advances in SIC are conferred. Chapter 3 has the critical presentation and analysis of the selected SIC methods from the literature. In Chapter 4, the simulations and its results are given. Chapter 5 presents the experimental setup and the experiment results and verification of it by simulations. Discussions and conclusion are made in the final Chapter 6.

CHAPTER 2

A SURVEY OF WIRELESS FULL DUPLEX

In this chapter a comprehensive survey of in-band full duplex is presented. The history of IBFD, starting from radars, recent advances, its applications and different self-interference cancellation methods are presented in detail.

2.1 A Brief History of In-band Full Duplex

In-band full duplex is known and used since 1940s in continuous wave (CW) radars; but up until recently it has not gained much attention in wireless data communications. In this section, the history of IBFD in radars and data communications are presented, separately.

2.1.1 Full Duplex Radars

CW radars do employ IBFD, such that, they transmit and collect (receive) the reflected signals simultaneously, in contrast to pulsed radars, which employ a fast switching between the transmission and reception, i.e. half-duplex. Self-interference in radar literature is often called "transmitter leakage" [20]. The CW radars of 1940s and 50s utilized a simple propagation domain approach to manage the self-interference: in bistatic radars, where the transmit and the receive antenna are separate, antennas were placed distant to increase the isolation (path loss) between them; in monostatic radars, where transmission and reception are done on one shared antenna, an isolator component, often circulator, was placed between the transmit and receive chains

to achieve some isolation between them. However, these methods can only supply a moderate amount of self-interference cancellation, therefore the transmit powers were kept small in order to keep the self-interference at a managable level. The small transmit powers, in turn, limited the range of CW radars. However, this range limitation was not a hindrance, because in close ranges the required switching period of pulsed radars were impractically low, so that only CW radars could be used for close range operation, i.e. the pulsed and CW radars complemented each other in operational range.

An analog domain SIC method, called "feedthru nulling", was proposed in 1960s [21]. 60 dB of SIC was reported there, however, the canceller itself weighed more than 60 kilograms using complex circuitry and it was very expensive. Coming to 1990s, [22] proposed an adaptive analog canceller, whose performance was demonstrated in [23]. Many improvements on SIC for monostatic CW radars have been proposed [24, 25, 26, 27, 28, 29, 30] . The reason that the efforts focus on monostatic rather than bistatic is that the isolation capacity of a built-for-the-purpose isolation component, e.g., circulator, hybrid coupler, etc., is superior and more controllable than a free space isolation as employed in bistatic configurations. Discussion on different antenna setups and propagation domain SIC is presented in Section 2.3.1.

2.1.2 Full Duplex Wireless Data Communications

The first data communication application to use IBFD was unidirectional forwarding, namely relaying. The relays in wireless data communications first receive then amplifiy and retransmit the received signal. Relays are generally used for coverage extension, e.g. in consumer home Wi-Fi applications, or to reach or hop over otherwise unreachable or impassable-by-wireline places, e.g. tunnels, difficult lands.

The early self-interference cancellation efforts in relays have tried to put antennas as far as possible, much like in bistatic CW radars, in order to manage the self-interference [31, 32, 33, 34]. Analog and digital domain SIC were tried as well [47, 35, 36, 37, 38, 39, 40]. Using antenna arrays for beamforming allowed for spatial SI nulling as well [41, 42, 43, 44, 45, 46, 47, 49, 50].

The information theoretic analysis of IBFD relaying is carried out in perfect SIC case in [53, 51, 52, 54, 55]; as well as in the presence of residual SI case in [56, 50, 57, 58, 59, 60, 61]. The other sources of impediments to IBFD are also studied information theoretically, e.g., channel estimation error, the limited dynamic range of ADC, and RF impairments in receive and transmit chains, in [49, 62].

Although an early and discontinued effort exists for bidirectional IBFD in [63], i.e., where two nodes exchange data, it was only the recent demand for high spectral efficiency for consumer applications such as Wi-Fi and cellular (4G, 5G) that has resulted in a huge wave of research efforts by the academic world and the industry towards implementing practical IBFD bidirectional wireless data communications. *Practical* is a critical term in this context, because this recent effort is concentrated on consumer applications, which brings the cost-performance balance, and many other considerations like operational environment and limited energy for battery powered mobile equipments. For example, high quality RF components, when used in transmit and receive chains of an IBFD radio, will alleviate the challenge against RF impairments such as mixer imbalances, oscillator induced issues (e.g. phase noise), and power amplifier distortion, but they are also too costly to be used in common consumer products. Also, a very complex and power hungry self-interference cancellation method can not find itself any use in energy limited mobile devices. In [64, 65, 66, 41, 67, 68, 69, 70] experiments demonstrated the feasibility of practical bidirectional IBFD, however, only in low transmit powers, i.e. short ranges, and under bandwidth constraints. But, in [71, 72, 73, 74] a better self-interference cancellation was accomplished and they demonstrated the feasibility of IBFD Wi-Fi. Subsequent research improved the SIC in [75, 76, 77, 78, 79]. Furthermore, numerous patents are already granted [80, 81, 82].

Another effort is concentrated on analyzing the bottlenecks of the IBFD in [76, 83, 84, 85, 86, 87, 88]. With theory and experiments combined, they tried to characterize the limitations to the IBFD to pave the way for improvements. Effects of RF impairments are extensively studied in [79, 89, 86, 90, 91, 92].

The in-band full duplex research is also in mutual interest with out-of-band full duplex interference management, because, for example, colocating the half-duplex and out-of-band full duplex devices on adjacent frequencies, or even using closely placed

time and frequency slots in half-duplex and out-of-band full duplex, respectively, will result in considerable interference. Such interference management is studied in [94, 95, 96, 97].

Multi user wireless networks have also their share in IBFD [54, 98, 99, 100]. Distributed IBFD is studied in [101, 102]; cognitive radios in [103]; and multiband systems in [104, 105].

IBFD beyond physical layer has also been studied. In [106, 107] medium access control (MAC) is studied; in [108, 109, 110, 111] cross layer network optimization in network scheduling. IBFD for neighbour discovery, mutual broadcasting, and localization are studied in [112],[113], and [114] respectively.

2.2 Applications of Full Duplex

In addition to the immediate and most prolific advantage of IBFD to double the link capacity, there are other usefull applications, too, presented in this section.

2.2.1 Doubling the Capacity

In bidirectional wireless data communications, assuming both nodes are IBFD, potentially, the link capacity can be doubled, assuming perfect SIC. This assumption may not always hold. However, a high amount of SIC can be achieved practically. Thus less than double, but still very high capacity gains are reported, which can be as high as 1.84, [79, 65, 15, 69].

2.2.2 Base Stations

In a multi user network (e.g. cellular), a base station (BS) serves several users. Just making the BS IBFD can gain the network much. In base station topologies, as much of the complexity and power consumption as possible is preferred to be on the BS rather than user equipment. So, it is likely and feasible that only the BS can be made full duplex. The main gain is that the BS can serve two users at the same time with

no additional time or frequency resources, as the same frequency band can serve as uplink and downlink to either user. Assuming that the inter-user interference is manageable, this application can save the network operator from paying for excessive expensive commercial spectrum. Another, and similar, application would be to use the same frequency band for backhaul communications, [115, 116].

2.2.3 Medium Access Control

In medium access control (MAC) layer, the biggest advantage of using IBFD is its solution to *hidden node* problem, an issue encountered in carrier sense multiple access networks. The simplest manifestation of this problem is as follows: in a three node one hop network scenario, in which only one node can access both nodes but other two nodes can not access each other directly, i.e. a line configuration, the hidden node problem can occur. The nodes that are unaware of (i.e. hidden to) each other can try to communicate simultaneously with the middle node, which has access to both, and result in a collision. If IBFD was to be used for only the middle node in such a scenario, the middle node can transmit a "busy" signal while receiving from either node, so that the node who wishes to transmit must first listen for "busy" signal and adjust its transmission accordingly. Reference [65] reported less collisions thus increased throughput this way.

2.2.4 Cognitive Radios

Collision issue in cognitive radios can be solved with IBFD as well. Cognitive radios use a frequency band as a secondary user and therefore whenever the primary user of that band communicates, it must cease its own communication as to not interfere (collide) with the primary user [117]. Traditionally, in time division duplexing, this interference is avoided by periodic listening of the channel for the primary user's communication. This traditional approach has two drawbacks, 1) the listening gap: if the channel was free, surely the listening time is wasted, 2) collisions: as this time division method has intervals when the channel is not listened to, a collision might happen anyway.

In IBFD cognitive radios, [65, 118, 119], a better interference avoidance and overall throughput increase is reported. In IBFD mode, instead of using the receiver as a means of data communications, it is used for spectrum sensing, and whenever a primary user is sensed, the transmission is ceased. It eliminates both drawbacks listed above efficiently.

2.2.5 Receiver Feedback

Feedback such as channel state information (CSI), acknowledgement/negativeacknowledgement can be delivered back from receiver to transmitter without having to wait for the transmission to end. In [120], it was shown that using IBFD bidirectional communications to exchange feedback, the gained benefit is more than the interference induced performance degradation.

2.2.6 Relaying

It was shown in [9, 10] that using IBFD can reduce the forwarding delay. Because the transmission and reception on the relay happens simultaneously, the delay observed from the source to destination through the relay can be reduced.

Out-of-band full duplex can, theoretically, achieve the same transmission/reception simultaneity but at the cost of using double the bandwidth and having to change the frequency band over the relay.

2.2.7 Wireless Secrecy

IBFD can help achieve better wireless network secrecy as well, as studied in [121, 122]. In this application, the receiving node transmits a jamming signal and at the same time receives a packet, that is wished to be kept private, from another node. The mixed signal, i.e. jamming signal plus the private packet, will be hard for any eavesdropper to correctly decode given that, as shown in [123], the jamming signal is of unknown structure. Hence the receiver knows the jamming signal it transmits, it can cancel it by SIC methods and decode the private packet successfully.

2.3 Self-interference Cancellation Methods

In this section, the three domain, propagation, analog, and digital, self-interference cancellation methods are discussed. Their individual and interactive analysis are carried out.

2.3.1 Propagation Domain

Wireless propagation domain SIC focuses on cancelling SI before it reaches the receive antenna and superposed on the intended received signal. The main reason for doing SIC in propagation domain is to alleviate the need for high dynamic ranges for receive chain components. Because, if the power of the intended received signal falls under SI more than the dynamic range, it will be lost. And, unfortunately, it is very likely to happen, because the intended received signal is much weaker than the SI at receive antenna. Another reason is to avoid the highly nonlinear region of the receiver low noise amplifier (LNA): the unusually high received signal power of the SI will drive the LNA into the nonlinear region, possibly even to saturation, hence heavily distort the whole received signal.

In separate antenna systems, the propagation domain SIC is done utilizing path loss [64, 65, 66, 72, 69], cross polarization [76, 72, 77, 80], or antenna directionality [76, 77]. In shared antenna systems, it is done by an isolating component between transmit and receive chains, generally a circulator.

In separate antenna configurations, the distant placement of the receive and transmit antennas, or utilizing an electromagnetic shield/absorber between the antennas are studied in [64, 76, 31, 69, 77]. Though these techniques are simple and effective, their use is limited by the device dimensions (form factor). Cross polarization, studied in [76, 68, 72] is another mean to achieve SIC. By making the transmit and receive antennas crossly polarized, ideally, one can avoid all interference. However it has its limitations, too. First of all, this technique constrains the degree of freedom for polarization utilization. Secondly, although the direct path between the two antennas will not alter the polarization much, the back scattered SI may change its polarization and limit the SIC capacity. In [75, 76] using directional transmit and receive antennas, i.e.

nonuniform radiation and reception fields, to create null fields for self-interference signal is studied. Antenna nulling is a similar approach that uses two transmit antennas to create a null point, and placing the receive antenna there suppresses the SI spatially [65, 66, 72, 80].

The spatial SIC methods discussed above are quite sensitive to device placement and implementation errors. However, it was shown in [76] using off the shelf equipment in an anechoic chamber (i.e. an electromagnetically clean and reflection free space) that more than 70 dB of spatial SIC can be achieved. Limitations to the frequency dependent methods, e.g. antenna nulling, are the carrier frequency reconfigurations and broadband signals. The methods discussed above exclusively focus on the line-of-sight (LOS)/direct path SI suppression, therefore when the power of reflected SI is moderately high, e.g. in a small confined reflective environment, the performance of these propagation domain techniques are diminished. Although in an anechoic chamber, which resembles a free outdoor environment, [76] has achieved 70+ dB SIC, in a small confined reflective environment it performed around 40 dB SIC. The reflected SI issue is also present in shared antenna configurations, while there is no way to discern the reflected SI superposed on intended received signal by propagation domain techniques.

In order to suppress the reflected SI, a propagation domain SIC taking into account the channel (i.e. channel aware) should be used. Transmit beamforming is such a method, that by adjusting the complex weights of the antennas in an array, it steers itself electronically to create SI nulls at receive antenna positions. Antenna nulling, mentioned above, is a static (channel unaware) and simple example of that, where two antennas are mechanically preadjusted (i.e., placed fixed) so that a predetermined point is null of SI for the receive antenna to be placed on. Such transmit beamforming is studied in [41, 44, 45, 46, 47, 124, 48]. Channel aware techniques, however, require channel knowledge to adjust the antenna weights. It can be retrieved either directly by channel estimation or nondirectly by adaptively adjusted weights. Creating nulls this way, requires more transmit antennas than receive antennas, because each null point eats up one degree of freedom in the weight vector of transmit array.

The propagation domain techniques may have altering effects on intended transmis-

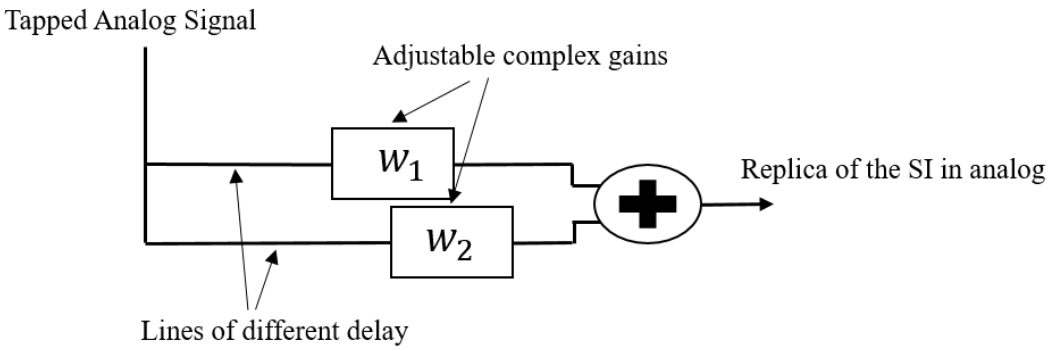

Figure 2.1: Analog transversal filter for SIC

sion and reception as well, e.g., by creating unwanted null fields or distorting the signals unintentionally, hence they should be designed taking into account the overall communication performance.

In this thesis, an analysis of a particular spatial SIC is not performed, rather, typical SIC values obtained in the literature experimentally or theoretically are adopted in calculations and simulations if they are deemed appropriate/applicable to the case and found to be realistic, which is around 20 - 30dB in most literature. In experiments, by using directional antennas and some moderate inter-antenna distance, spatial SIC around 30 dB is achieved.

2.3.2 Analog Domain

Analog domain SIC is a subtractive SIC method performed before the received signal reaches the ADC of the receive path. The transmit SI signal is tapped from the transmit chain. The exact point of tapping is relevant as discussed below. After being processed, it is subtracted from the received signal somewhere in the receive chain, the exact point of subtraction is relevant as in tapping but must be before ADC, in order to cancel out the SI component in the mixed received signal. Tapping of the transmit SI as close as possible to the transmit antenna has the advantage of involving all the RF impairment effects and noise of the transmit chain readily in the signal, therefore they do not need to be dealt with separately. From the tapping point to the subtraction point, the channel seen by the SI is estimated and applied to the tapped signal so that the subtrahend signal matches the received SI as close as possible. The subtraction

point should be as close as possible to the receive antenna to decrease the dynamic range of the received signal, therefore alleviating the constraint on dynamic ranges of receive chain components. Although an analog baseband SIC approach exists [125], typically the subtraction takes place before the LNA, in passband. In [64, 71, 73] the transmit SI is tapped in digital baseband and after applying the estimated channel response in digital baseband, where it is easier to do so than in analog passband, it is upconverted by an additional RF chain to be subtracted from the received signal. This digital-processing-then-upconverting approach, however, has the drawback of having to estimate the transmit chain response of the SI and vulnerability to impairments in the upconverting cancellation RF chain. Figure 2.1 shows the basic two-tap analog domain SIC filter. It takes the tapped signal, applies delays and weights to it to match it with the received SI and outputs the replica of the transmit SI. The delay lines are generally fixed and predefined. The complex gains are adjusted generally adaptively.

2.3.3 Digital Domain

Digital domain SIC is a subtractive SIC method, which uses the tapped digital baseband transmit SI to cancel out the received SI from the total received signal after it is converted to digital by ADC. In digital domain, the tools available to the designer are much more efficient and plentiful than in analog. The main limitation to it is the dynamic range of the ADC, which determines the maximum amount of digital domain SIC achievable. The biggest attractiveness of the digital SIC is its availability: every digital communications system has some sort of digital signal processing capability that can be partitioned for digital SIC; unlike propagation and analog domain SIC where dedicated devices should be built exclusively for self-interference cancellation. Ideally, the digital SIC can achieve infinite suppression of self-interference in the absence of the random noise [87]. Another advantage of relying on digital methods is the booming computation power.

The digital SIC methods start by building a system model that models everything between the transmit digital-to-analog converter (DAC) and receive ADC. The transmit chain can distort the digital baseband signal from the DAC to the transmit antenna with quantization noise, upconverter phase noise, mixer imbalances and high-power

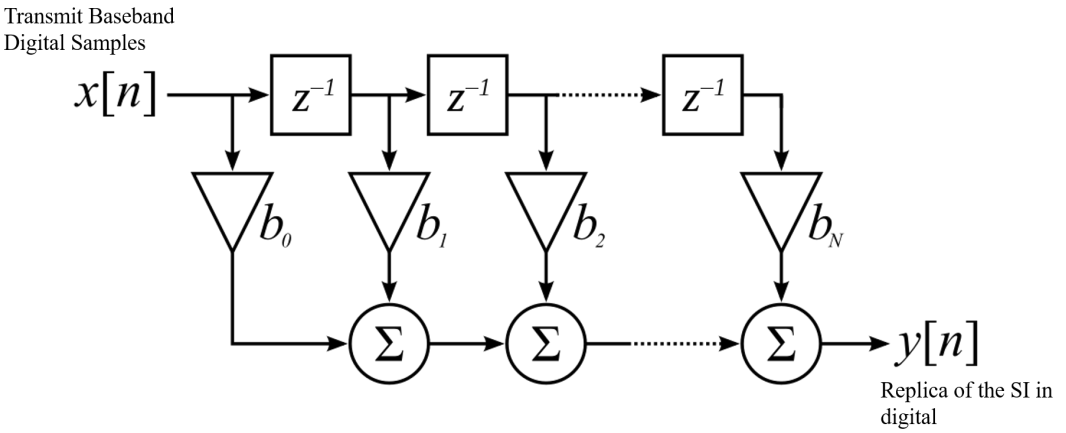

Figure 2.2: Digital FIR filter for SIC

amplifier nonlinearities [126]. Some distortions listed here may require nonlinear signal processing to cope with. The receive chain, likewise, has the capability to distort the signal in the same manner as the transmit chain. The propagation path between the antennas must be modelled accurately as well. A highly reflective environment with long delay spread for broadband signals is highly problematic, for example. The model should also take into account the preceding SIC methods' (propagation and analog domain) effects as well.

In [127], the effect of mixer imbalances are studied. In [79, 91, 128] nonlinear power amplifier distortion is studied. In [87] the phase noise is explicitly studied. [129] integrates the two RF impairments, viz., the mixer imbalances and power amplifier nonlinearities, to cope with them jointly. In [136], adaptive SIC is studied experimentally for mobile device scenarios.

In Figure 2.2, the digital SIC filter is shown. It is pretty much a conventional FIR filter. Its weights can be adjusted either adaptively or non-adaptively.

The next chapter will present, in detail, the analog and digital self-interference methods we have evaluated and tested in this thesis study.

CHAPTER 3

SELF-INTERFERENCE CANCELLATION

In this chapter, selected self-interference cancellation methods in analog and digital domains from the recent literature are critically presented, commented on, and therefrom some extensions are derived.

3.1 Analog Domain Self-Interference Cancellation

In this section, a subtractive analog SIC method is studied. In this method, the transmit SI signal is tapped from the transmit chain in analog domain. It is tapped, preferably, as close as possible to the transmit antenna in order for it to contain all the RF imperfections of the transmit chain, so that they do not have to be estimated by the SIC mechanism. The channel response from the tapping point to the subtraction point is then estimated by adaptive means. Then, the channel response is applied to the tapped signal by an analog transversal filter. This filter, usually, has multiple predetermined delay lines and adjustable complex gains. Output of the analog filter is desired to be a replica of the received SI. This replica is, then, subtracted from the total received signal, in an effort to suppress the received SI without deteriorating the intended received signal. A realistic assumption is that the intended received signal sent by the other node is not correlated with the self-interference, so that the subtractive cancellation will not suppress the intended received signal as well, unintentionally.

The method proposed in [92] is the basis for analog domain cancellation studied in this thesis. Much like [79], it taps the signal at the output of the transmit power amplifier just before the transmit antenna and passes it through a multiple-delay-line

tunable analog filter, which mimics the channel seen by the SI signal. At the receive side, it is subtracted from the total received signal just after the receive antenna. Reference [92]'s main advantage over [79] is that that it uses complex gains in the transversal filter in contrast to real gains of the latter. An analog transversal filter has multiple delay lines and adjustable weights, as shown in Figure 2.1. Using real gains requires more delay lines to adjust the phase of the tapped signal correctly. The delay lines are the biggest space consumers on a board so the minimum amount of them should be used for small form factor devices, i.e., mobile. Its performance, as a variant demonstrated experimentally in [130], is quite good even for very wide band signals. In simulations, it can achieve up to 100 dB of cancellation but in experiments it can achieve around 50 dB of cancellation. In the rest of this section, analysis of the aforementioned paper is carried out. Reproduction of some of the material from [92] is provided here for the convenience of the reader.

3.1.1 System Model and MMSE Solution

The transmit signal (SI) in passband can be written as

$$\begin{aligned} x(t) &= Re\left\{(x_i(t) + jx_q(t))e^{-j\omega t}\right\} \\ &= x_i(t)cos(\omega t) + x_q(t)sin(\omega t) \end{aligned} \tag{3.1}$$

where $Re\{\cdot\}$ represents the real part of $\cdot$, ω is the carrier frequency in radians per second, and $x_i(t)$ and $x_q(t)$ are the baseband inphase and quadrature components of the transmit signal, respectively. Without loss of generality, assuming a single path of SI coupling into the receive chain, the received signal can be written as [92]

$$y(t) = g\, x(t-\tau) + r(t) + n(t) \tag{3.2}$$

where g and τ are the unknown gain and delay of the SI, respectively, $r(t)$ is the intended received signal sent by the other nodes and $n(t)$ is the additive white Gaussian noise (AWGN). The proposed method of the paper cancels the self-interference by taking multiple replicas of $x(t)$ and apply complex gains and delay to them to estimate the SI by their linear combination. Using two taps, the estimated SI can be written as [92]

$$e(t) = w_{1i}x(t-\tau_1) + w_{1q}\tilde{x}(t-\tau_1) + w_{2i}x(t-\tau_2) + w_{2q}\tilde{x}(t-\tau_2) \tag{3.3}$$

where w_{ki} and w_{kq} are the inphase and quadrature components of the kth tap weight and $\tilde{x} = x_i(t)sin\omega t - x_q(t)cos(\omega t)$ is the Hilbert transform of $x(t)$ and τ_k is the delay of the k-th filter tap. The job of the SI canceller is to find the gain values that cancels the SI most. The delays τ_k are taken to be fixed, e.g., a fixed length microstrip line, so the optimization of the cancellation with respect to tap delays should be carried out by the designer before manufacturing the actual circuit with delay lines. Then the output of the subtractive canceller can be written as

$$z(t) = y(t) - e(t) \tag{3.4}$$

In [92], it is proposed to transform the passband model to the equivalent baseband model in order to simplify the derivations of the tap weights. This means also putting downconverters and upconvertes in the analog circuitry. The transmit signal in baseband can be written as

$$X(t) = x_i(t) + jx_q(t) \tag{3.5}$$

Then, from (3.2) subsequently, the received signal in baseband equivalent form is

$$Y(t) = gX(t-\tau)e^{j\omega\tau} + R(t) + N(t) \tag{3.6}$$

where $R(t)$ and $N(t)$ complex baseband equivalents of the intended received signal and AWGN, respectively. Similarly, the output of the canceller in baseband is

$$Z(t) = Y(t) - W_1X(t-\tau_1)e^{j\omega\tau_1} - W_2X(t-\tau_2)e^{j\omega\tau_2} \tag{3.7}$$

In vector notation

$$Z(t) = Y(t) - \mathbf{W}^T\mathbf{X}(t) \tag{3.8}$$

where $(\cdot)^T$ represents transpose, $\mathbf{W} = [W_1W_2]^T$, where $W_k = w_{ki} + jw_{kq}$, and $\mathbf{X} = [X(t-\tau_1)e^{j\omega\tau_1}X(t-\tau_2)e^{j\omega\tau_2}]^T$. Implementation of the optimum minimum mean squared error (MMSE) solution in the analog domain is deemed impossible in the paper, but they provide the MMSE solution anyhow to provide insight to the performance of the canceller. In MMSE, the output of the canceller, (3.8), is minimized, and assuming that the transmit signal $x(t)$ and the intended received signal $r(t)$ are uncorrelated, and along with the uncorrelated noise $n(t)$, this will only minimize the SI since only the tapped SI is preknown and fed to the canceller. The cost function that minimizes the SI is given as

$$\min_{\mathbf{W}} E\left\{|Z(t)|^2\right\} = \min_{\mathbf{W}} E\left\{\left|Y(t) - \mathbf{W}^T\mathbf{X}\right|^2\right\} \tag{3.9}$$

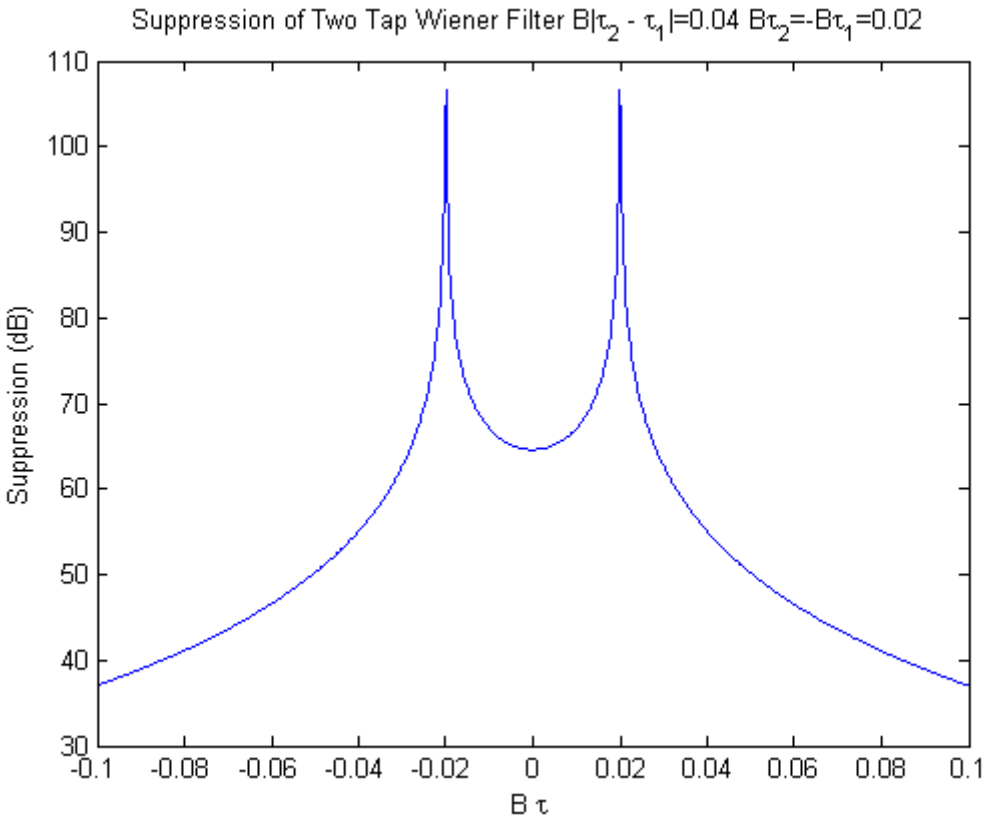

Figure 3.1: Effect of the delay of received SI path on suppression. B=20MHz.

where the suppression equals to

$$\begin{aligned} Suppression &= \frac{Received\ SI\ Power}{Residual\ SI\ Power} \\ &= \frac{E\left\{|gX(t-\tau)|^2\right\}}{E\left\{\left|gX(t-\tau)e^{j\omega\tau} - \mathbf{W}^T\mathbf{X}(t)\right|^2\right\}} \end{aligned} \tag{3.10}$$

The suppression is not a function of carrier frequency or received SI strength, rather it depends on the delay difference between taps and the number of taps used, as shown in [92]. In Figure 3.1 the suppression of the two tap MMSE filter is presented. The taps are positioned 2 nanoseconds apart, as in [130]. The maximum suppression occurs when the delay of the received SI coincides with one of the delay lines. The suppression is more graceful when the received SI falls between the taps, but degrades faster outside the tap delays.

In a two tap MMSE filter, addition of another received SI path, e.g., a reflected path, is studied next. Adding a second path, the received SI signal, disregarding the intended

received signal and noise, can be written as

$$Y_2(t) = X(t-\tau)e^{j\omega\tau} + X(t-\tau-\delta)e^{j\omega(\tau+\delta)+\theta} \tag{3.11}$$

where δ is the second SI path delay and θ is its arbitrary phase.

The power of $Y_2(t)$ is then, assuming $E\left\{|X(t)|^2\right\} = 1$,

$$E\left\{|Y_2(t)|^2\right\} = 2(1 + cos(\omega\delta + \theta)sinc(B\delta)) \tag{3.12}$$

Depending on the sign of the cosine term, the second SI path can reduce the total SI power. However, this is a phenomenon that is hard to exploit; even when the second SI path is coming from within the device, a much more controlled environment. The first reason therefore is, it is very much frequency and implementation accuracy dependent. Secondly, even assuming that the second path is the reflected SI from the antenna caused by impedance mismatch in a shared antenna configuration, the reflection coefficient of the antenna must be predetermined, so that its sign does not change during operation. This is another relatively difficult engineering problem. Finally, the reflected power should be in close proximity of that of the first SI path, so that a considerable cancellation can occur. In order to neglect this phenomenon, in [92], $cos(\omega\delta + \theta) = 1$ is assumed and $sinc(B\delta) > 0$, i.e., the second SI path is not very far from the first, so the effect of an additional SI path is considerably negative on suppression performance.

The suppression of two tap MMSE filter for two SI paths is derived in [92]. Depicted in in Figure 3.2, shows the suppression performance of the two tap MMSE filter under two SI paths, one is coincided on the left tap, and the other is varying. As compared to the one path performance, there is some performance loss but, overall, the suppression level is still high.

3.1.2 Adaptive Analog SI Cancellation

As applying the MMSE solution in analog domain is not an option, the authors of [92], apply the steepest descent method to the cost function (3.9). This is a well known solution, when direct application of the MMSE filter is not possible, [131].

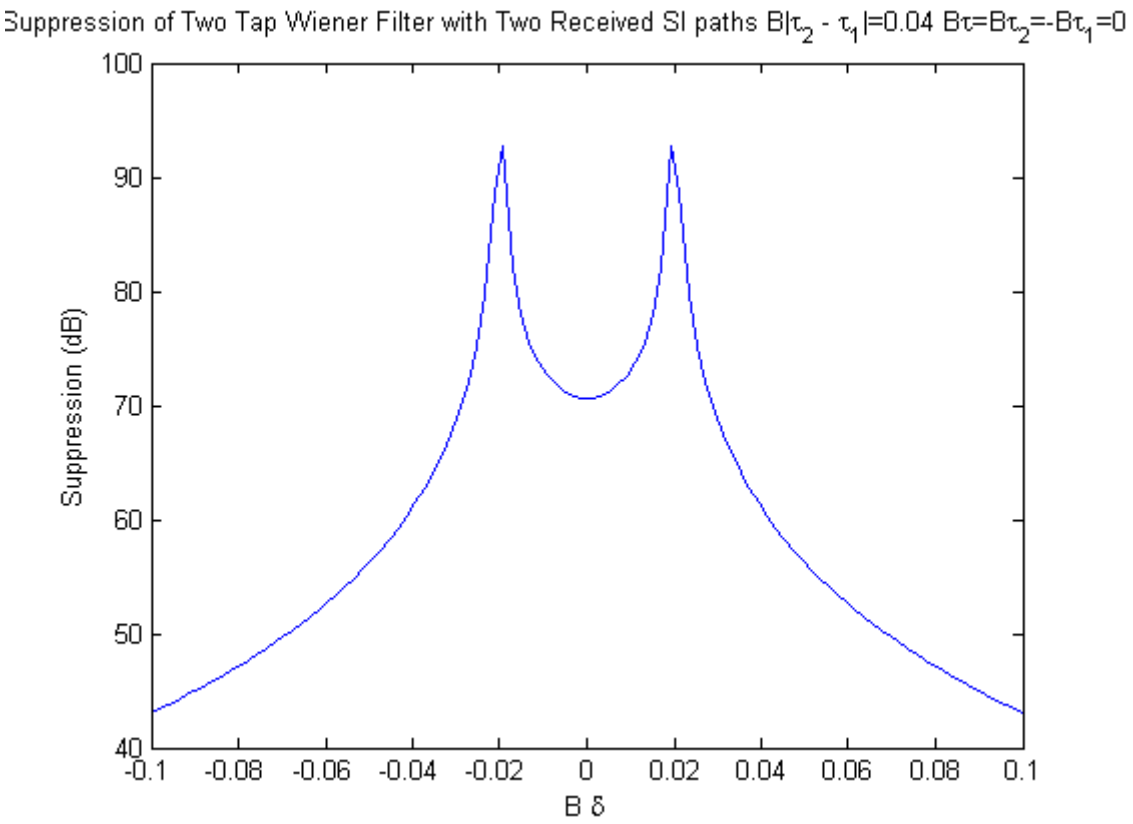

Figure 3.2: Effect of the delay of a second received SI path on suppression. First path delay is at $B\delta = -0.02$, so it coincides with the delay line. B=20MHz.

The tap weights W_k can be adaptively calculated by (modified from [92], as discussed below)

$$\begin{aligned} W_k &= W_k - \frac{\mu}{2}\frac{\partial |Z(t)|^2}{\partial W_k} \\ &= W_k + \mu \{X_k^*(t)Z(t)\} \\ &= W_k + \mu[(x_i(t)z_i(t) + x_q(t)z_q(t)) + j(x_i(t)z_q(t) - x_q(t)z_i(t))] \end{aligned} \tag{3.13}$$

where μ is a real, non-negative constant, often defined as step size. The delay applied by the k-th tap is omitted here.

In [92], the implementation of the adaptive filter is proposed to be carried out by parallel phase shifters in each tap, instead of the Hilbert transform as introduced in (3.3), that consequently resulted in (3.13), because, as they argue, an implemented analog Hilbert transform would not make the inphase and quadrature components exactly orthogonal but a combination of parallel phase shifters would control the phase applied by the filter better. In practice, using parallel phase shifters, where each

would require its own downconverter, would be impractically complex to implement on a small or medium form factor analog board, and there is no direct implementation of it to the best of our knowledge. In [92], the tap weights were real and phase shifting of the tapped SI was accomplished by adjusting the real gains of paralled phase shifters. An implemented method directly using (3.13) exists. In [130], using vector modulators the complex weights are directly applied to the tapped SI.

The tap weights calculated in (3.13) are first passed through an integrator, because typically they are too noisy, so the integrator suppresses their noise, and then the step size is applied, generally a small constant, governed by the stability considerations of the adaptive filter [131].

After taking into account the delay of each tap, the filter weights of the k-th tap are calculated explicitly by

$$\begin{aligned} w_{ki} &= w_{ki} + \mu \int [x_i(t-\tau_k)z_i(t) + x_q(t-\tau_k)z_q(t)]dt \\ w_{kq} &= w_{kq} + \mu \int [x_i(t-\tau_k)z_q(t) - x_q(t-\tau_k)z_i(t)]dt \end{aligned} \tag{3.14}$$

where τ_k is the delay applied by the k-th tap.

3.2 Digital Domain Self-Interference Cancellation

Subtractive digital domain self-interference cancellation methods tap the transmit SI from the digital baseband and after applying the channel response as seen by the SI from transmit DAC to receive ADC, subtracts the processed tapped SI, which is now a replica of the received SI in digital, from the total received signal in digital. The principle is the same as in analog domain, but digital domain offers more tools to the designer in implementing the self-interference cancellation. Some methods incorporate nonlinear signal processing, as well, in order to capture the effect of the nonlinear devices, such as power amplifiers. This section is divided into two: 1) static channels and 2) dynamic channels, where the latter utilizes adaptive filters, the former uses nonadaptive methods.

3.2.1 Static Channels

In this section the digital domain self-interference for static channels are studied. [129] is chosen as the basis model for digital SIC, because it incorporates and jointly handles two of the most SIC performance degrading RF impairments, viz., the nonlinearities mainly induced by power amplifiers (PA) and image signals mainly caused by unbalanced processing of inphase and quadrature components of the SI by the mixers. The outer-device channel from the transmit antenna to the receive antenna is assumed to be static in this analysis. This can correspond to any immobile or nearly-immobile scenario, e.g. base stations, a modem in a large confined space, etc.

3.2.1.1 Baseband Equivalent Signal Model

The transmit signal (SI) in discrete time complex baseband can be written as

$$x[n] = x_i[n] + jx_q[n] \tag{3.15}$$

where n is the sample index. When this baseband signal is modulated and fed to the mixer (i.e. IQ modulator), the output in discrete time complex baseband can be written as [129]

$$x^{IQM}[n] = K_1 x[n] + K_2 x^*[n] \tag{3.16}$$

where $K_1 = 0.5(1 + g\ exp(j\varphi))$ and $K_2 = 0.5(1 - g\ exp(j\varphi))$, where g and φ are the gain and phase imbalance of the mixer, respectively. In typical RF front-ends, $|K_1| \gg |K_2|$. The quality of an RF front-end in this context can be quantified by its image rejection ratio defined as $10\log_{10}(|K_1|^2 / |K_2|^2)$.

The assumed model for the transmit power amplifier is the parallel Hammerstein (PH) model. The output of the power amplifier is given by [129]

$$x^{PA}[n] = \sum_{\substack{p=1 \\ p\ odd}}^{P} \sum_{m=0}^{M} h_p[m]\psi_p(x^{IQM}[n-m]) \tag{3.17}$$

where the basis functions are defined as [129]

$$\psi_p(x[n]) = |x[n]|^{p-1}\, x[n] = x[n]^{\frac{p+1}{2}} x^*[n]^{\frac{p-1}{2}}, \tag{3.18}$$

$h_p[m]$ are the FIR filter coefficients of the PH model for the p-th order nonlinearity branch, and M and P are the memory depth and nonlinearity order of the PH model, respectively. [132, 133, 134, 135] have shown that the PH model can accurately model the behaviour of RF power amplifiers.

Combining (3.16), (3.17) and (3.18), the output of the PA can be written as

$$x^{PA}[n] = \sum_{\substack{p=1 \\ p\ odd}}^{P} \sum_{q=0}^{p} \sum_{m=0}^{M} h_p^{q,p-q}[m] x[n-m]^q x^*[n-m]^{p-q} \tag{3.19}$$

where $h_p^{q,p-q}[m]$ are the combined coefficients of the PA and mixer. This model has, surely, many coefficients to be estimated, however, most of these terms will be negligibly small as higher order nonlinear terms and images have small powers, their combinations will have even smaller powers.

Note that, at this stage the basis function to be used in the channel estimation is established as $x[n-m]^q x^*[n-m]^{p-q}$. After this stage, only the coefficients of the FIR filter that is applied by the channel to this basis are to be determined.

3.2.1.2 Channel and Analog SIC Effect

The outer-device channel and the analog self-interference canceller are put into the model, as well. The received SI can be written as, at the receiver antenna [129, (5)]

$$z[n] = \sum_{l=0}^{L} c[l] x^{PA}[n-l] \tag{3.20}$$

where $c[l]$ are the FIR coefficients of the actual physical (outer-device) channel, and L is its memory depth.

After the reception, the analog canceller comes into play and the signal after the canceller can be written as [129]

$$\begin{aligned} r[n] &= z[n] - \sum_{l=0}^{L'} h^{RF}[l] x^{PA}[n-l] \\ &= \sum_{\substack{p=1 \\ p\ odd}}^{P} \sum_{q=0}^{p} \sum_{m=0}^{M+max(L,L')} \overline{h}_p^{q,p-q}[m] x[n-m]^q x^*[n-m]^{p-q} \end{aligned} \tag{3.21}$$

where $\overline{h}_p^{q,p-q}[m] = \sum_{l=0}^{m} c^{RF} h_p^{q,p-q}[m-l]$, $c^{RF}[l] = c[l] - h^{RF}[l]$, and $h^{RF}[l]$ are the tap weights of the analog domain canceller. L' is the number of taps in the analog SIC.

3.2.1.3 Comment on Basis Functions

The basis functions' contribution to the SI will be depending on the channel response, as seen above. When implementing the actual digital canceller, the designer should analyse this, and select the basis functions which contribute the most, because the negative effect of estimation noise induced by the weak basis functions can be larger than their contribution to the accuracy of the SI estimation.

3.2.1.4 SI Canceller Structure

Now, the task of the digital domain self-interference canceller is to estimate the $\overline{h}_p^{q,p-q}[m]$ terms and apply them to the corresponding basis functions obtained through the tapped digital baseband SI and subtract the replicated SI from the received signal.

The total received signal in discrete time complex baseband can be written as

$$y[n] = r[n] + s[n] + w[n] \tag{3.22}$$

where $r[n]$, from (3.21), is the residual SI after analog domain cancellation, $s[n]$ is the intended received signal sent by other nodes, and $w[n]$ is the additive white Gaussian noise. All these components of the received signal are assumed to be uncorrelated.

The output of the digital SIC is then

$$\hat{s}[n] = y[n] - \hat{r}[n] \tag{3.23}$$

where $\hat{r}[n]$ is the estimated SI.

3.2.1.5 SI Estimation

In vector notation, the signal at the input of the digital domain canceller is

$$\begin{aligned} &\mathbf{y} = \mathbf{r} + \mathbf{s} + \mathbf{w}, \\ &\mathbf{y} = [y[n]\ y[n+1]\ \cdots y[n+N-1]]^T \end{aligned} \tag{3.24}$$

where N is the number of observed samples, and the other vectors can be written in the same manner as $y[n]$.

The estimation error is then defined as [129]

$$\boldsymbol{e} = \boldsymbol{y} - \hat{\boldsymbol{r}} \tag{3.25}$$

where the estimate is given as

$$\hat{\boldsymbol{r}} = \boldsymbol{\Psi}\hat{\overline{\boldsymbol{h}}} \tag{3.26}$$

with $\boldsymbol{\Psi}$ being the horizontal concatenation of the matrices

$$\boldsymbol{\Psi}_{\mathbf{q},\mathbf{p}} = \begin{bmatrix} \psi_{q,p}[n] & \psi_{q,p}[n-1] & \cdots & \psi_{q,p}[n-\overline{M}+1] \\ \psi_{q,p}[n+1] & \psi_{q,p}[n] & \cdots & \psi_{q,p}[n-\overline{M}+2] \\ \vdots & \vdots & \ddots & \vdots \\ \psi_{q,p}[n+N-1] & \psi_{q,p}[n+N-2] & \cdots & \psi_{q,p}[n+N-\overline{M}] \end{bmatrix}, \tag{3.27}$$

$\psi_{q,p}[n] = x[n]^q x^*[n]^{p-q}$, with $p = 1, 3, \ldots, \overline{P}$, and $q = 0, 1, 2, \ldots, p$, and $\overline{P}$ and $\overline{M}$ are the selected nonlinearity order and memory depth, respectively.

The estimated channel vector $\hat{\overline{\boldsymbol{h}}}^{q,p-q}$ is the vertical concatenation of the vectors

$$\hat{\overline{\boldsymbol{h}}} = [\hat{\overline{h}}_p^{q,p-q}[0]\ \hat{\overline{h}}_p^{q,p-q}[1]\ \ldots\ \hat{\overline{h}}_p^{q,p-q}[\overline{M}-1]]^T \tag{3.28}$$

The channel vector $\hat{\overline{\boldsymbol{h}}}$ is then found to be the solution to the minimization of the norm square of error vector $\boldsymbol{e}$, i.e., least-squares solution, [129]

$$\begin{aligned}\hat{\overline{\boldsymbol{h}}} &= \arg\min_{\overline{\boldsymbol{h}}} \|\boldsymbol{e}\|^2 = \arg\min_{\overline{\boldsymbol{h}}} \left\|\boldsymbol{y} - \boldsymbol{\Psi}\overline{\boldsymbol{h}}\right\|^2 \\ &= (\boldsymbol{\Psi}^H\boldsymbol{\Psi})^{-1}\boldsymbol{\Psi}^H\boldsymbol{y}\end{aligned} \tag{3.29}$$

assuming a full rank $\boldsymbol{\Psi}$.

3.2.2 Dynamic Channels

In dynamic channel environments, based on the simplified signal model of [129], [136] proposed an adaptive scheme using the least mean squares (LMS) algorithm. Although, they did not test their algorithm under dynamic channel environments, we did test it and got satisfactory results as seen in simulations in Chapter 4.

In this section, the LMS algorithm of [136] is presented, then its variants, normalized-LMS (NLMS) and RLS are derived and presented consecutively. LMS and RLS are the two most common adaptive estimation algorithms. Details on their theoretical background and comparison of them can be found in detail in [131].

3.2.2.1 LMS Adaptive Filter

As stated in [131], the LMS algorithm is popular mainly because of its simplicity. Acting on current estimation error fed back to the adaptive filter weight calculation block, LMS recursively (and "hopefully", [131]) converges to a statistically good level of estimation accuracy; in our case the estimated SI.

In the basis functions, different from [129], [136] omits the mixer induced impairments manifested as image signals.

The new basis functions, involving only the PA induced nonlinearities, can be written as

$$\boldsymbol{\Psi}(n) = [\psi_1((x)n)\ \psi_3((x)n) \cdots\ \psi_P((x)n)]^T \tag{3.30}$$

where $\psi_p(x(n)) = |x(n)|^{p-1}\, x(n)$, as in (3.18). P is the assumed maximum nonlinearity order of the signal basis.

The tapped SI fed to the filter at index n is defined as [136]

$$\mathbf{u}(n) = [\mathbf{\Psi}(n)^T \ \mathbf{\Psi}(n-1)^T \ \mathbf{\Psi}(n-2)^T \ \cdots \ \mathbf{\Psi}(n-M+1)^T]^T \tag{3.31}$$

where M is the memory depth of the adaptive filter.

The channel vector to be estimated adaptively by the filter is defined as [136]

$$\mathbf{h}(n) = [h_1(0) \ h_3(0) \ \cdots \ h_P(0) \ h_1(1) \ \cdots \ h_P(M-1)]^T \tag{3.32}$$

Parameters: Memory length of the adaptive filter ($M = M_{pre} + M_{post} + 1$) and step size μ

Data: Basis functions $\mathbf{u}(n)$ and received signal $y(n)$

Output: The canceller output signal $e(n)$

begin

Initialize: $\mathbf{h}(0) = 0$, $n = M_{post}$

while *transmitting* **do**

$\mathbf{u}(n) = [\mathbf{\Psi}(n + M_{pre})^T \ \mathbf{\Psi}(n + M_{pre} - 1)^T \ \cdots \ \mathbf{\Psi}(n - M_{post})^T]^T$;

$e(n) = y(n) - \mathbf{h}^H(n)\mathbf{u}(n)$;

$\mathbf{h}(n+1) = \mathbf{h}(n) + \mu\mathbf{u}(n)e^*(n)$;

$n = n + 1$;

end

Algorithm 1: LMS algorithm, [136]

In Algorithm 1, the output $e(n)$ contains both the residual SI, left from estimation error, and the intended received signal as well, so it will be fed directly to the decoder for the decoding of the intended received signal.

3.2.2.2 Normalized LMS Adaptive Filter

When the eigenvalue spread of the input vector $\mathbf{u}(n)$ is large, as it is in our case, as shown in [136], the LMS algorithm performance degrades. The dominant bases shadow the others, since the error vector $e(n)$ is just a scalar and does not include the filter tap-wise error [131]. One way of overcoming this is the NLMS, which normalizes the input vector $\mathbf{u}(n)$ in every iteration, so the otherwise shadowed bases can also contribute to the adaptation of the filter weights.

Parameters: Memory length of the adaptive filter ($M = M_{pre} + M_{post} + 1$) and step size μ

Data: Basis functions $\mathbf{u}(n)$ and received signal $y(n)$

Output: The canceller output signal $e(n)$

begin

Initialize: $\mathbf{h}(0) = 0$, $n = M_{post}$

while *transmitting* **do**

$\mathbf{u}(n) = [\mathbf{\Psi}(n + M_{pre})^T \ \mathbf{\Psi}(n + M_{pre} - 1)^T \ \cdots \ \mathbf{\Psi}(n - M_{post})^T]^T$;

$e(n) = y(n) - \mathbf{h}^H(n)\mathbf{u}(n)$;

$\mathbf{h}(n + 1) = \mathbf{h}(n) + \frac{\mu}{\|\mathbf{u}(n)\|^2}\mathbf{u}(n)e^*(n)$;

$n = n + 1$;

end

Algorithm 2: NLMS algorithm, [131]

The NLMS algorithm is the same in every step but the normalization step, compared to LMS, but it is given here in full for completeness. In Algorihm 2, the $\|\cdot\|$ refers to the Euclidean norm.

3.2.2.3 RLS Adaptive Filter

RLS is a recursive approach to the least-squares solution, [131]. It is described in Algorithm 3. The regularizing term σ there, is a positive constant, which is taken to be small when the SNR is high, and large when the SNR is low. When uncertain, it can be taken as unity, as by the adaptive nature of the filter it will be forgotten anyhow. Forgetting factor λ is a positive constant less than unity, typically taken to be close to unity. It governs the rate at which the past affects future weights, a unity forgetting factor means no forgetting at all, also called windowed RLS. The details of derivation of the intermediate steps can be found in [131].

Parameters: Memory length of the adaptive filter ($M = M_{pre} + M_{post} + 1$), forgetting factor λ and regularizing term σ.

Data: Basis functions $\mathbf{u}(n)$ and received signal $y(n)$

Output: The canceller output signal $e(n)$ $e(n)$

begin

Initialize: $\mathbf{h}(0) = 0$, $n = M_{post}$ and $\mathbf{P}(0) = \sigma^{-1}\mathbf{I}$

while *transmitting* **do**

$\mathbf{u}(n) = [\mathbf{\Psi}(n + M_{pre})^T \ \mathbf{\Psi}(n + M_{pre} - 1)^T \ \cdots \ \mathbf{\Psi}(n - M_{post})^T]^T$;

$\boldsymbol{\pi}(n) = \mathbf{P}(n-1)\mathbf{u}(n)$;

$\mathbf{k}(n) = \frac{\boldsymbol{\pi}(n)}{\lambda + \mathbf{u}^H(n)\boldsymbol{\pi}(n)}$;

$e(n) = y(n) - \mathbf{h}^H(n-1)\mathbf{u}(n)$;

$\mathbf{h}(n) = \mathbf{h}(n-1) + \mathbf{k}(n)e^*(n)$;

$\mathbf{P}(n) = \lambda^{-1}\mathbf{P}(n-1) - \lambda^{-1}\mathbf{k}(n)\mathbf{u}^H(n)\mathbf{P}(n-1)$;

$n = n + 1$;

end

Algorithm 3: $\mathbf{I}$ is the identity matrix. RLS algorithm, [131]

CHAPTER 4

SIMULATION RESULTS

In this chapter, the methods proposed in Chapter 3 are tested in simulations. For the analog domain cancellation Advanced Design System (ADS) is used and for the digital domain methods Matlab/Simulink is preferred. Schematics and codes are presented in appendices.

4.1 Analog Domain Simulations

For a two tap analog cancellation filter, described in Section 3.1.2, a performance evaluation is carried out. The used signal is, conforming to IEEE 802.11n, OFDM with 20MHz bandwidth and QPSK constellation. It has 64 total subcarriers, of which 52 are data. A transmit power of 20dBm is assumed. A natural isolation of transmit and receive antennas of 20dB is assumed, which brought the received SI signal strength to 0dBm on average. The intended received signal is not present in this simulations, only the absolute suppression of the SI is evaluated. Conforming to the simulation parameters of [92], 3 dB of noise figure is assumed for the active components in the analog cancellation circuit. Gain and phase imbalances are 0.2% and 0.2 degrees, respectively, between the transmit and receive chain, [17]. Also, the downconverters noise figure are assumed to be 5 dB. There is also a nonlinear power amplifier after the transmit signal generation which has 10 dBm of IIP3. The channel is assumed to be static. The receiver noise floor is at -100dBm. The schematics of the ADS design are presented in Appendix A. All figures in this analog domain simulations section are taken from ADS.

The difference between the delay lines were taken to be 2 nanoseconds, and in the first case, only one SI path was produced to coincide with the first delay line. In the second case, 2 SI paths, with equal power, 2 nanoseconds apart were produced to each coincide with either delay lines, much like the experimental setting in [130].

In the first case, shown in Figure 4.1 and 4.2, an average of 80 dB cancellation was achieved. The spectrum is calculated at steady state, taken to be after 10 microseconds. In the second case, depicted in Figure4.3 and Figure4.4, an average of 60 dB cancellation was achieved. These results verify the findings of [92] and [130].

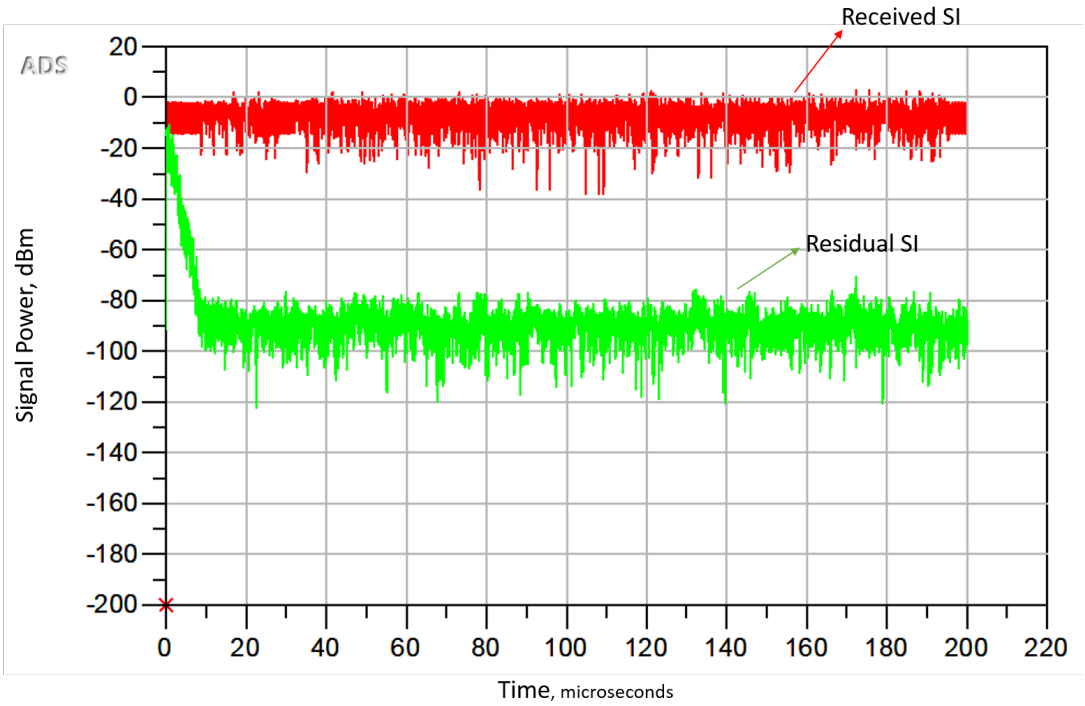

Figure 4.1: Received SI and the residual SI after analog SIC in two tap filter with one received SI path.

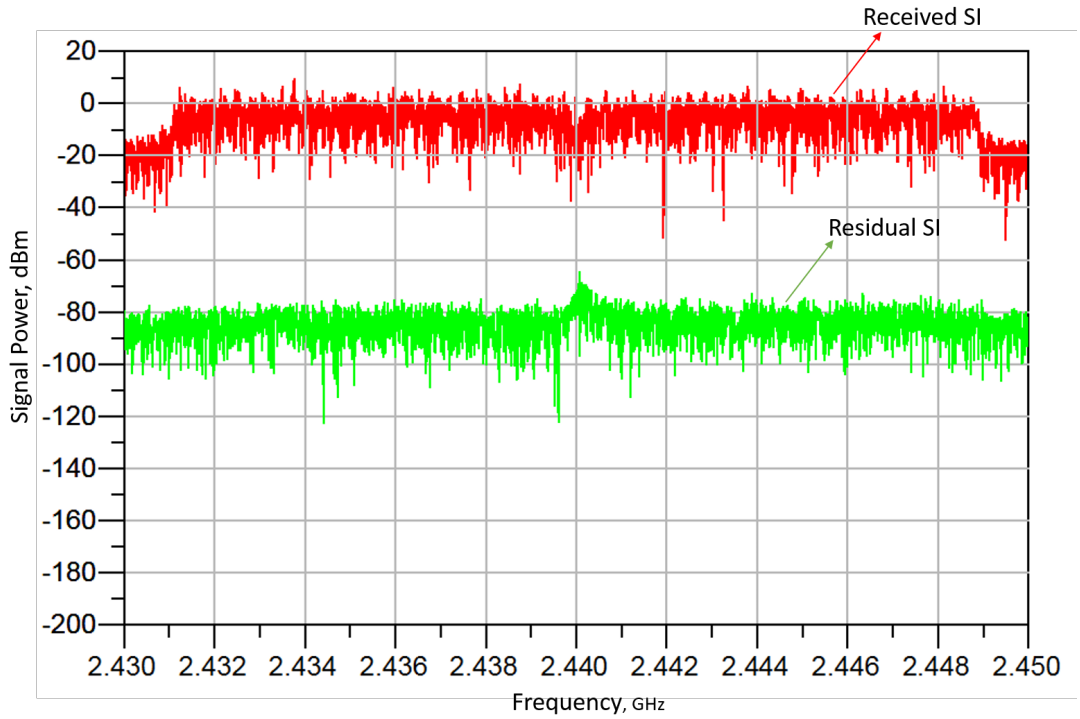

Figure 4.2: Spectrum of received SI and the residual SI after analog SIC in two tap filter with one received SI path.

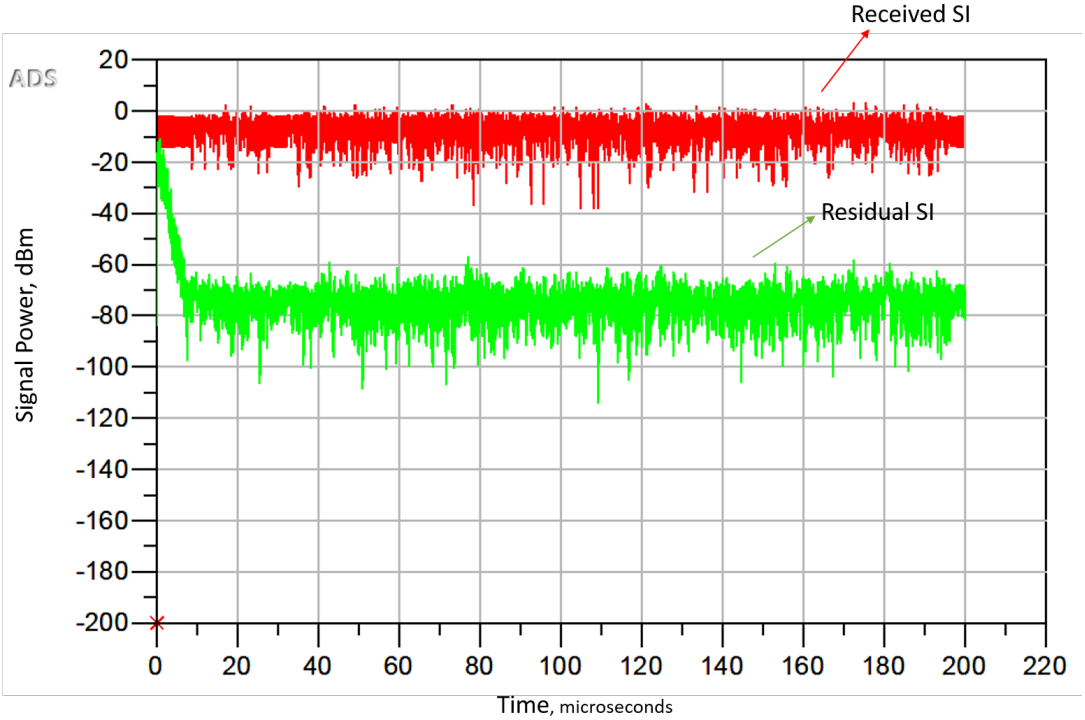

Figure 4.3: Received SI and the residual SI after analog SIC in two tap filter with two received SI paths.

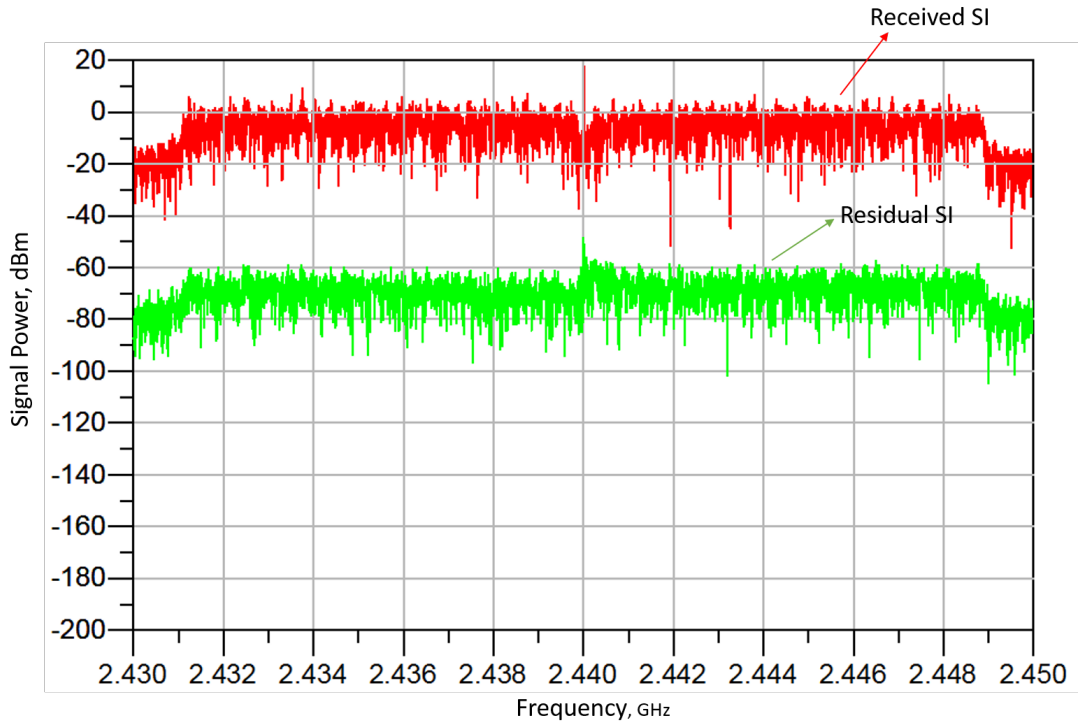

Figure 4.4: Spectrum of received SI and the residual SI after analog SIC in two tap filter with two received SI paths.

4.2 Digital Domain Simulations

In this section the results of digital domain SIC is presented in two parts: 1) static channels, 2) dynamic channels. All work in this section is carried out in Matlab/Simulink environment. The concerning simulation schematics are presented in Appendix B. All figures in this digital domain simulations section are taken from Matlab.

4.2.1 Static Channels

In the simulations, the intended received signal is assumed to have 15 dB SNR (in the absence of SI), which corresponds to -85 dBm signal power, with the -100 dBm receiver noise floor assumed. A separate antenna configuration is assumed with Rician fading with a K-factor of 35 dB, line-of-sight gain -30 dB and channel length $L = 3$, [71]. The channel is time-invariant. 10000 samples were used in each simulation run, repeated 10 times. Not much deviation between runs were observed. The PA model

Parameter	Value
Constellation	Rectangular 16-QAM
Number of total subcarriers	1024
Number of active subcarriers	512
Signal Bandwidth	10MHz

Table 4.1: Signal parameters used in testing

Parameter	Value
Rx NF	4 dB
Antenna Separation	30 dB
Analog Cancellation	30 dB
PAPR	10 dB
Tx IRR	25 dB
Rx IRR	50 dB
Rician Fading K factor	35 dB

Table 4.2: Simulation Parameters

is assumed to be PH, so no modelling mismatch is present. Also, the effect of RF cancellation is simulated. A two tap analog canceller provided 30 dB of SIC. This value is kept intentionally at this moderate level to test *alone* the digital cancellation better. Simulation environment parameters are provided in Table 4.2.

The RF impairments are listed in Table 4.3. The main source of the nonlinearity is the transmit power amplifier. Although a 25 dB of image rejection ratio (IRR) for the transmit mixer is assumed [137], it is just the minimum amount suggested by ETSI. Typically 50 dB of IRR can be achieved in widely used transceivers like AD9361, [17].

The simulated signal parameters are listed in Table 4.1. Rectangular 16-QAM was used in an OFDM signal with 1024 total and 512 active subcarriers, which corresponds to a roughly 2 times oversampling in time domain. The signal bandwidth was 10 MHz.

Component	Linear Gain (dB)	IIP2 (dBm)	IIP3 (dBm)	NF (dB)
PA (Tx)	27	-	13	4
LNA (Rx)	25	-	5	4
Mixer (Rx)	6	50	15	4

Table 4.3: Component Figures

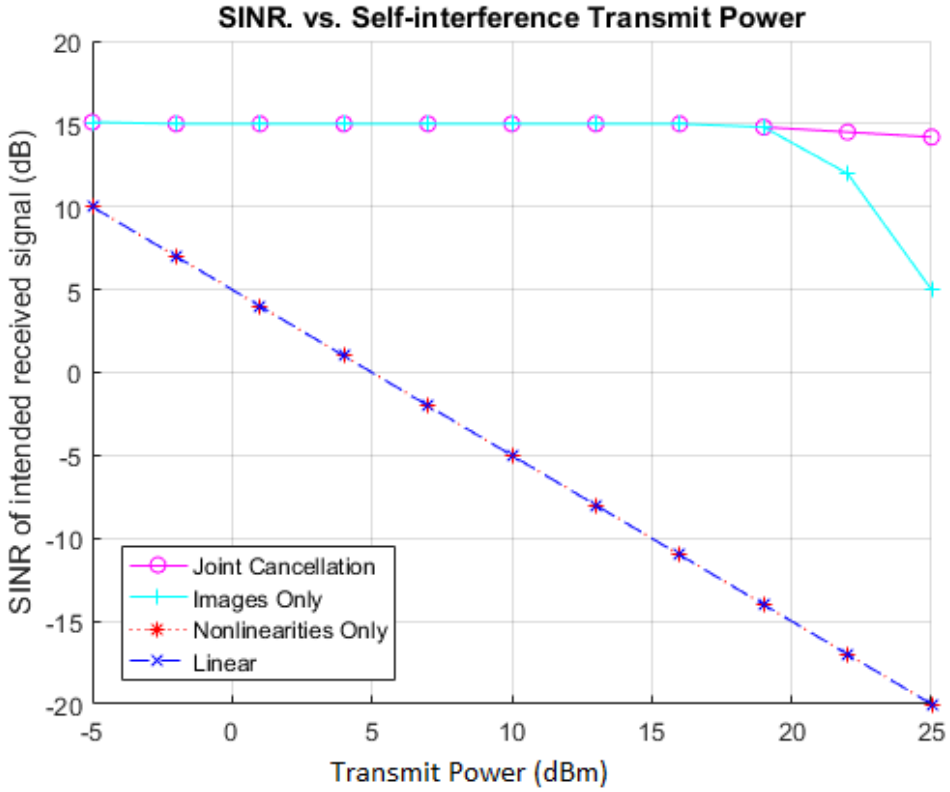

Figure 4.5: Performance comparison of different digital cancellation models. Image rejection ratio (IRR) is 25 dB, so images dominate SI.

In the first test, the intended received signal's signal-to-noise-plus-interference-ratio (SINR) against the transmit power of self-interference is studied. The assumed maximum nonlinearity order is $\overline{P} = 7$, and memory depth is $\overline{M} = 4$. The performance of the joint cancellation of nonlinearities and image signals; image signals only; nonlinearities only; and linear model are presented in Figure 4.5. With IRR of 25dB, the image signals dominate the SIC, so any cancellation not taking them into account (the bottom two) is sure to fail. The joint and only images can be discriminated only in very high transmit powers, where higher order nonlinear terms start to contribute more.

IRR is taken as 50 dB, and the same test is repeated, this time, for the joint cancellation and nonlinear only cancellation, to see whether they discriminate. There is no significant discrimination between the nonlinear only and joint cancellation, as shown in Figure 4.6.

With the first test parameters, IRR=25 dB, the strength of the received signal bases are presented in Figure 4.7. This analysis would be carried out in order to determine which bases should be used for estimation of the SI. In our case, the bases of component index>13, which correspond to after seventh order nonlinearity, do not contribute much. The effect of chosen maximum nonlinearity and memory depth is also studied. Figure 4.8 shows the effect of chosen maximum nonlinearity, $\overline{P}$. In Figure 4.9, the effect of assumed memory depth of the filter, $\overline{M}$, is presented, when the actual channel length in simulation was $M = 4$.

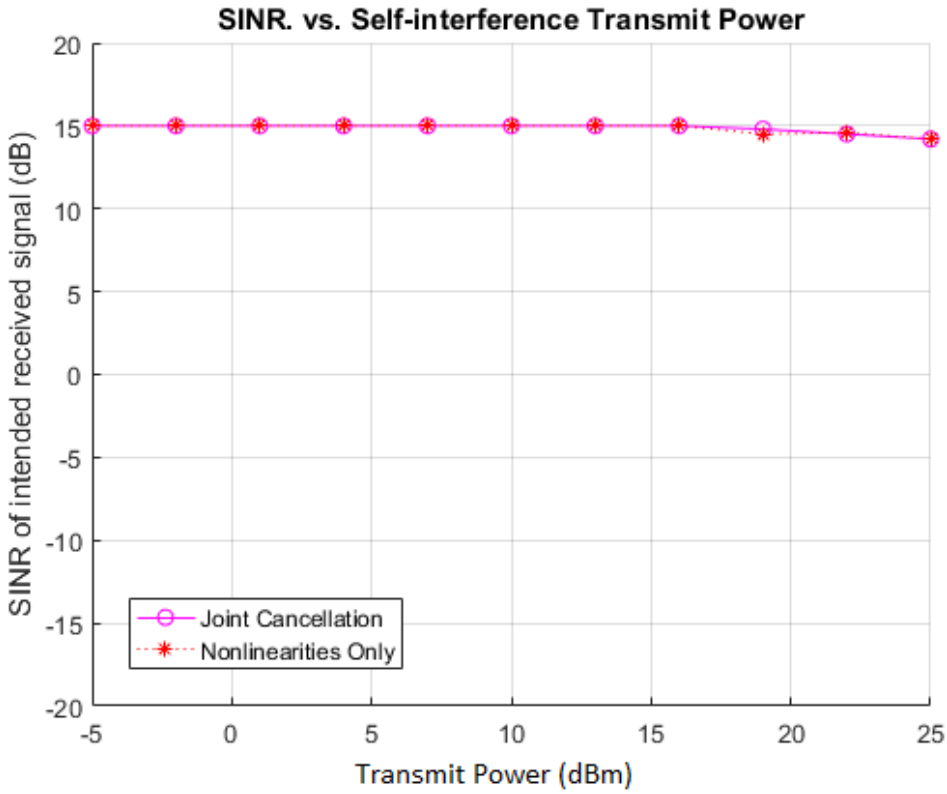

Figure 4.6: Performance comparison of the Joint and Nonlinear Only models. Image rejection ratio (IRR) is 50 dB, so they perform equally well.

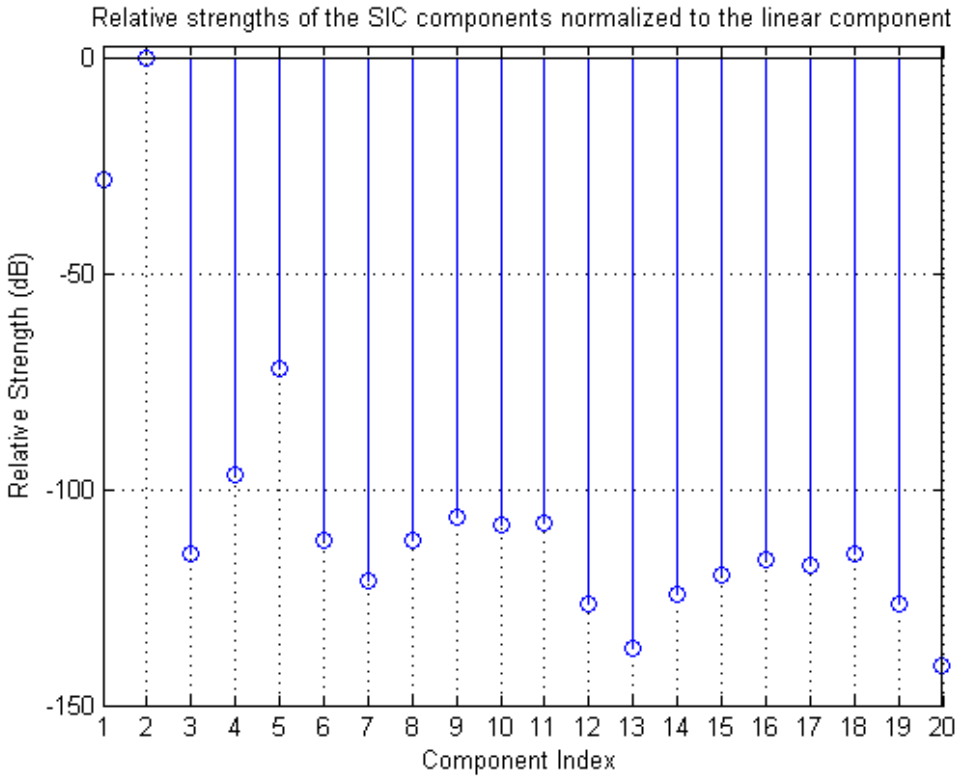

Index	1	2	3	4	5	6	7	8	9	10	11	12	13	14	15	16
k	0	1	0	1	2	3	0	1	2	3	4	5	0	1	2	3
j	1	0	3	2	1	0	5	4	3	2	1	0	7	6	5	4

Index	17	18	19	20
k	4	5	6	7
j	3	2	1	0

Figure 4.7: $x^{*j}x^k$. Signal bases' relative power, as formulated in the table above. j is the power of the conjugate and k is the power of linear term.

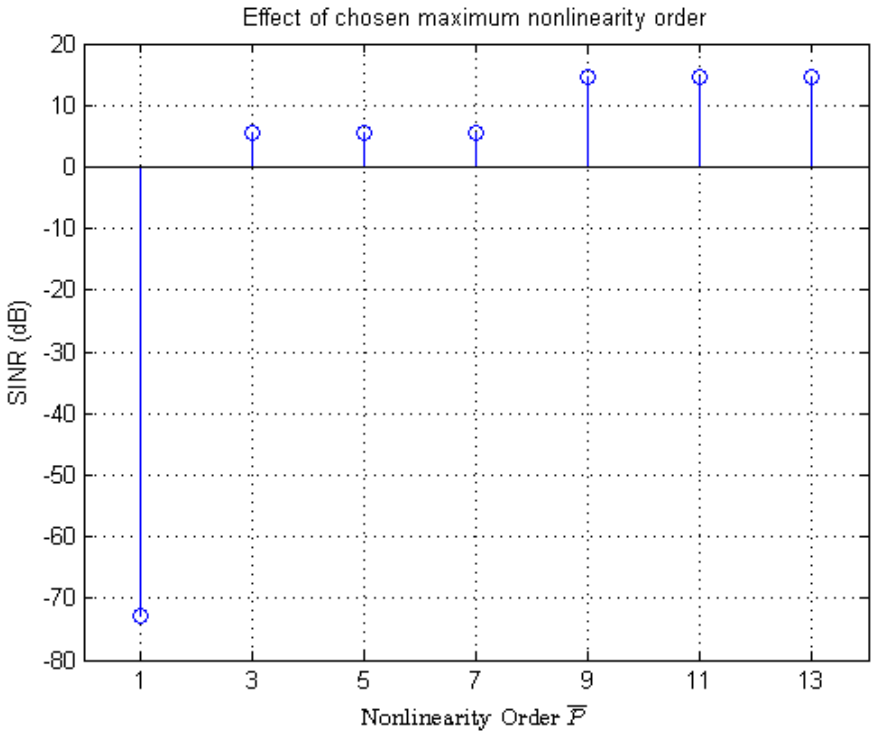

Figure 4.8: Effect of mismatch between the nonlinearity order of the cancellation model and simulation parameters.

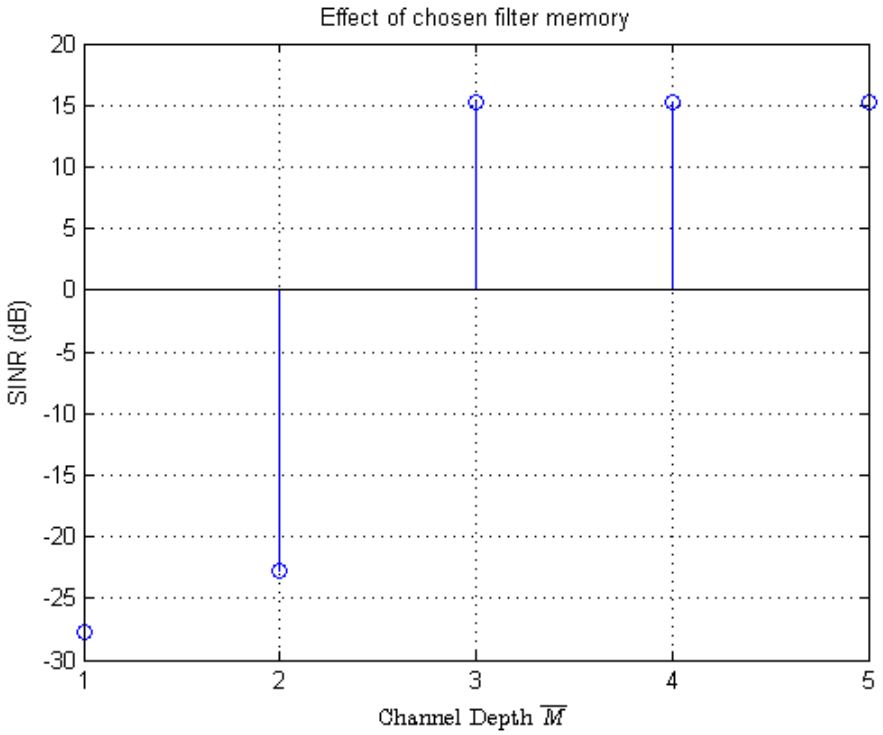

Figure 4.9: Effect of mismatch between the memory length of the cancellation model and simulation parameters.

4.2.2 Dynamic Channels

Simulations for dynamic channel environment are carried out with the same parameters as in Section 4.2.1, except: mixer induced image signals are not present in the bases, only the nonlinearity of PA is present; the channel is time variant; the simulations are run once but longer to observe the convergence of adaptive filters.

The same structure of Rician channel as above is assumed, but now with 10 Hz maximum Doppler frequency with Jakes spectrum type, which is equivalent to approximately 4kmph speed, which is the average walking speed of a person. The observed number of samples correspond to 100 OFDM symbols, so that $N = 102400$. Assumed maximum nonlinearity order is $\overline{P} = 7$ and the assumed memory depth is $\overline{M} = 4$. All proposed adaptive algorithms, viz., LMS, NLMS, and RLS, are tested comparatively. The intended received signal is present as above, and it is equalized with a zero-forcing equalizer, and its EVM is measured against time. As was in the case of static channels, there is 30 dB of analog cancellation and 30 dB of antenna isolation before the digital cancellation.

In Figure 4.10, the adaptive filters' EVM performances are presented. The target is -15 dB, as measured in the absence of interference. All adaptive filter parameters were judiciously optimized. The minimum steady-state error is favored against convergence speed, so in the LMS variants the step size μ was very small and in the RLS, the forgetting factor was almost unity, $\lambda = 0.9994$. Although there are some advices towards the stability and performance improvements for adaptive filters in [131], there is no strict rule on the parameter values. As experimentally observed, the minimum disturbance principal should be adopted, because aggressive adaptation, although provides rapid convergence, can affect the decoding performance of the intended received signal negatively.

An example time and frequency domain observation of the RLS adaptive filter are presented in Figure 4.11 and Figure 4.12, respectively. The spectrum is computed after steady state is reached. After steady-state, an average of 50 dB of digital SIC is achieved, which brought the SI almost down to the noise floor.

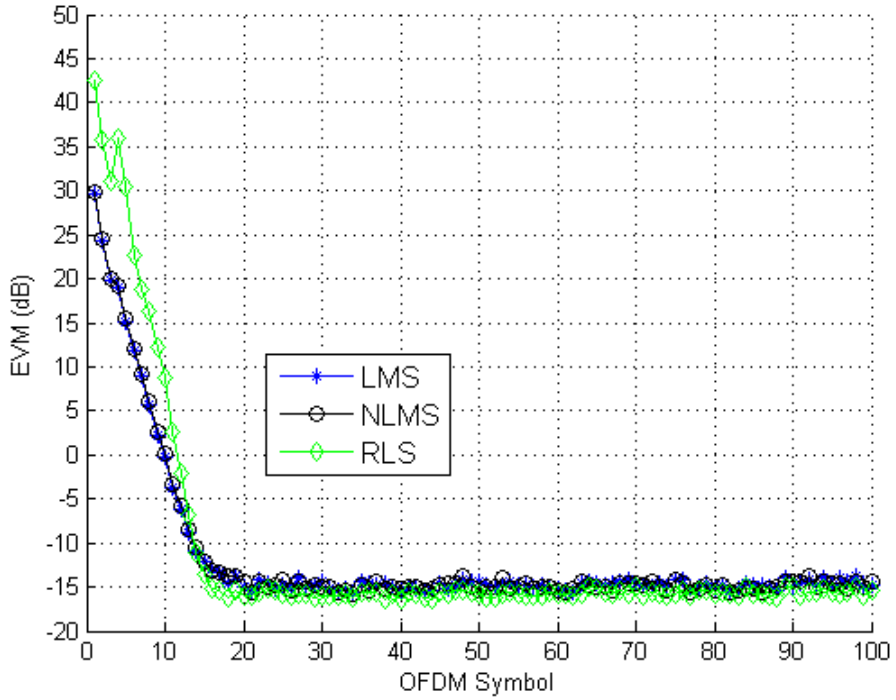

Figure 4.10: Performance comparison of different adaptive algorithms. The bound for EVM is -15 dB, that is the EVM of intended received signal without any interference.

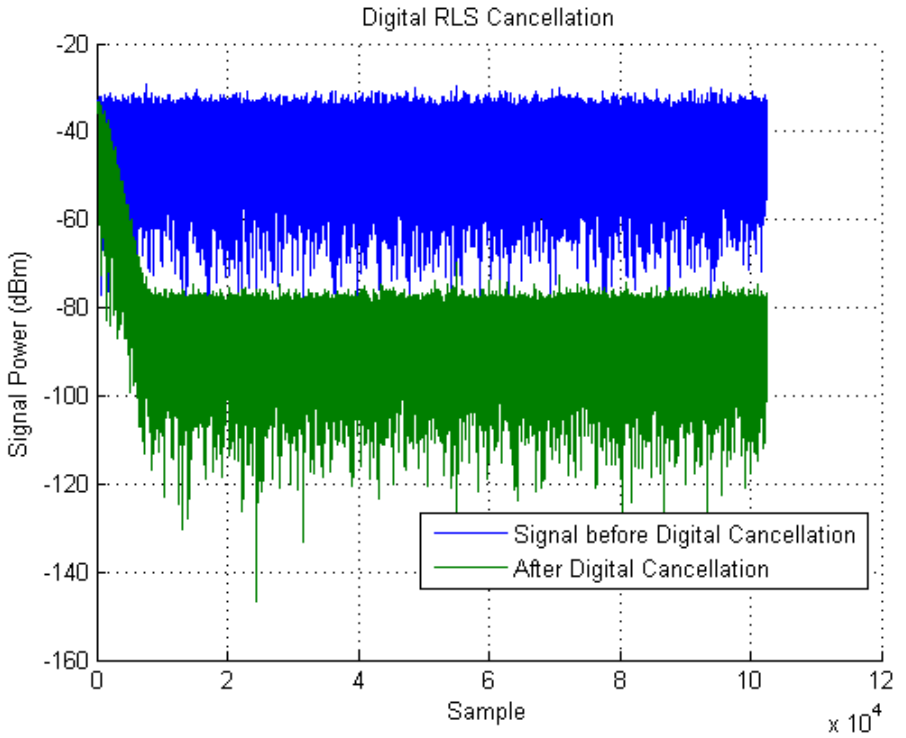

Figure 4.11: SI before and after digital RLS adaptive cancellation. 50 dB of cancellation is achieved.

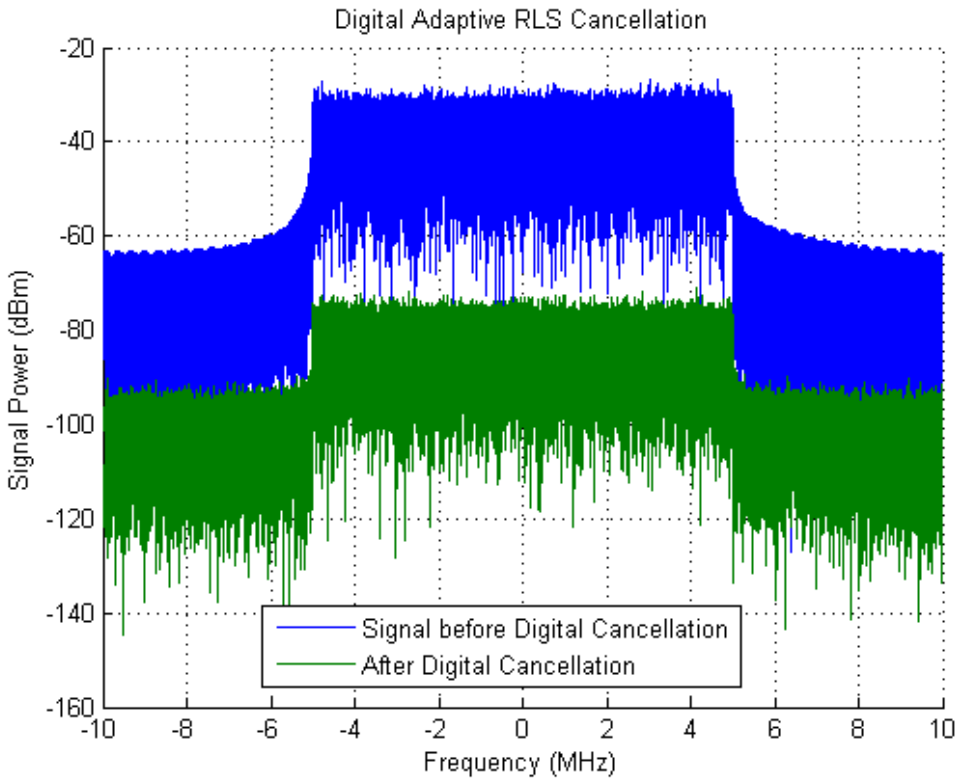

Figure 4.12: Spectrum of SI before and after digital RLS adaptive cancellation, as calculated after steady-state is reached.

CHAPTER 5

EXPERIMENTS

In this chapter, the experiments of an in-band full duplex transceiver are presented. Only propagation domain and digital self-interference cancellation method described in Section 3.2.1 were employed; there was no analog self-interference cancellation. The experiment setup is presented with a visual. The results indicate a bottleneck: phase noise. Verification and in-depth analysis of the experiment results are made via simulations using experimental parameters.

5.1 Experiment Setup

In the experiments, AD9361 RF transceiver, [17], with the evaluation board AD-FMCOMMS3-EBZ and evaluation kit Xilinx Zynq-7000 All Programmable SoC ZC702 was used. There are 2 transmit and 2 receive chains on the transceiver. The transmit chains share the same local oscillator with each other; likewise the receive chains among themselves. There was no option to make the transmit and receive chains to share the same local oscillator, which, as explained later, worsens the phase noise problem, which was the bottleneck for the digital cancellation. As full duplex requires, we activated one transmit path and one receive path at the same time and at the same carrier frequency. Separate antenna configuration was assumed. The nonuniform radiation pattern of the used patch antennas and their placement resulted in a spatial isolation (path loss) of approximately 32 dB (measured). A photograph of the experiment setup can be seen in Figure 5.1. The test environment was a medium size office.

The signal used, conforming to the general structure of 802.11ac, was an OFDM with 64 total subcarriers. A standard packet was formed and sent and received repeatedly for approximately 25 packets duration. Each packet was treated separately for self-interference cancellation and their results were averaged at the end. The preamble of the packet consisted of a short and a long training field, which consist of 2 repeated OFDM symbols and one OFDM symbol, respectively. Cyclic prefix length was 16. The payload (data part) of the burst (packet) consisted of 400 OFDM symbols. The constellation used was rectangular 16 QAM. The carrier frequency was chosen as 2.5 GHz. The data was recorded and sent to a PC to be processed offline in MATLAB.

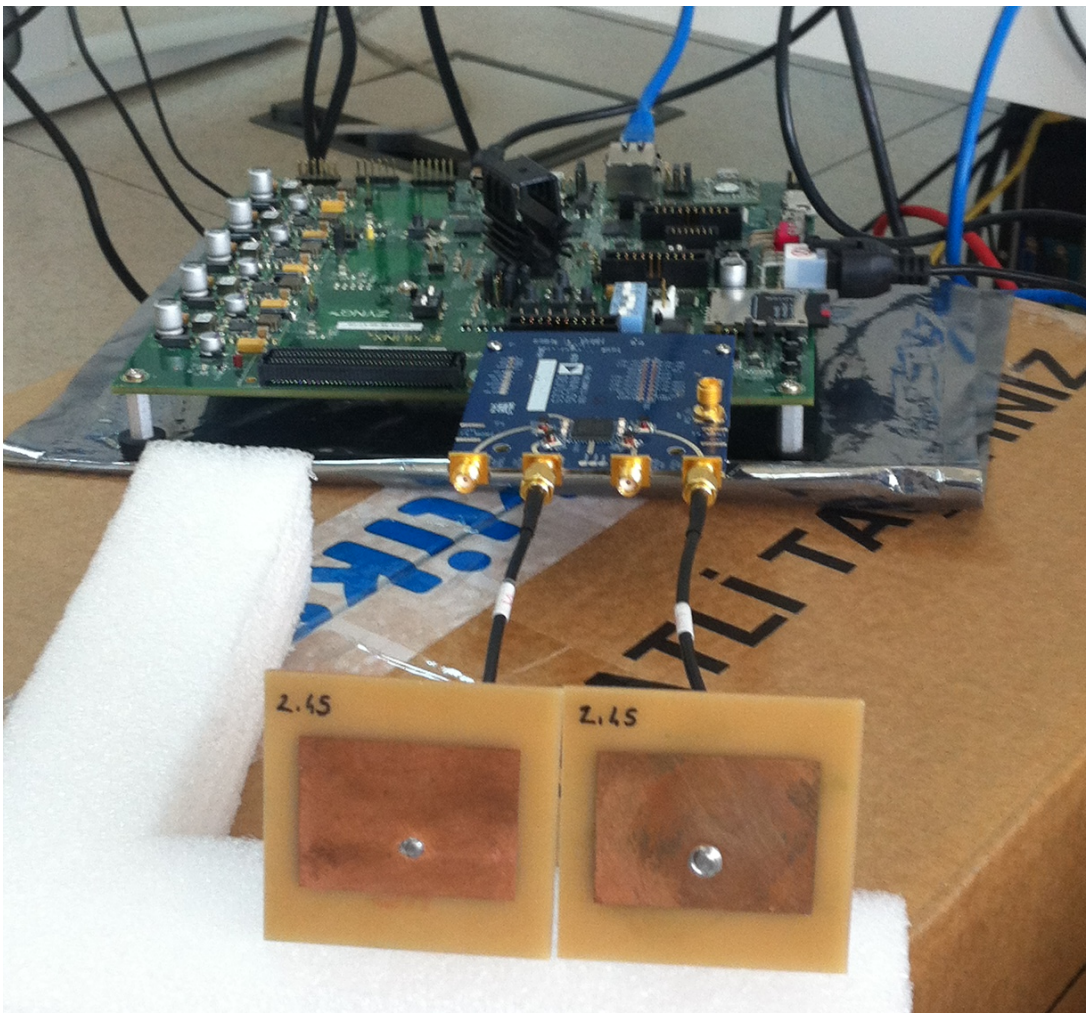

Figure 5.1: Experiment Setup

5.2 Experiment Results

The results of the first experiment can be seen in Figure 5.2. The average transmit power of the self-interference signal was swept from the maximum amount of approximately -6 dBm to the minimum level where the signal detection was possible. The receive path gain was adjusted to give the best response (i.e. linearity, dynamic range, etc.) for the self-interference signal, which meant lowering it to the unreccommended low levels at high received powers. The noise figure of the receive path as a whole, although not very linearly, is inversely proportional to the receive path gain. As a result, at high received self-interference powers, because of the used low receive path gains to avoid saturation, noise figures up to 15 dB are observed. This is observable as the increase of apparent noise floor. The digital cancellation was done with the algorithm described in Section 3.2.1. The transmit signal denoted as x there, is the transmit signal we feed the transceiver here; and the received signal y there, is the output of the ADC of the receiver path here. The cancellation algorithm is run for each packet separately and then the resultant cancellation performances are averaged for demonstration here. The assumed memory depth was $\overline{M} = 5$ and highest nonlinearity order was $\overline{P} = 5$. At transmit self-interference powers lower than approximately -30 dBm, cancellation of self-interference to the noise floor was accomplished. It should be noted that, we employed no form of analog domain cancellation. The amount of achievable analog cancellation can be added to the transmit power to shift it right by the graph. In other words, cancellation of self-interference up to the noise floor is possible at transmit SI powers of -30 dBm plus the ammount of achievable analog cancellation, which can be up to 80 dB, as shown in Section 4.1. Considering the maximum amount of allowed transmit power for indoor devices around 20 dBm, the complete cancellation of self-interference is possible for practical uses with a combination of propagation, analog and digital domain SIC.

The effect of assumed memory depth on cancellation is investigated in Figure 5.3. The number of taps used in channel estimation is increased from one to five. After the third tap is added, there was no considerable change. This memory effect comes from within the device as explained in the earlier chapters, because there was no reflector in the vicinity.

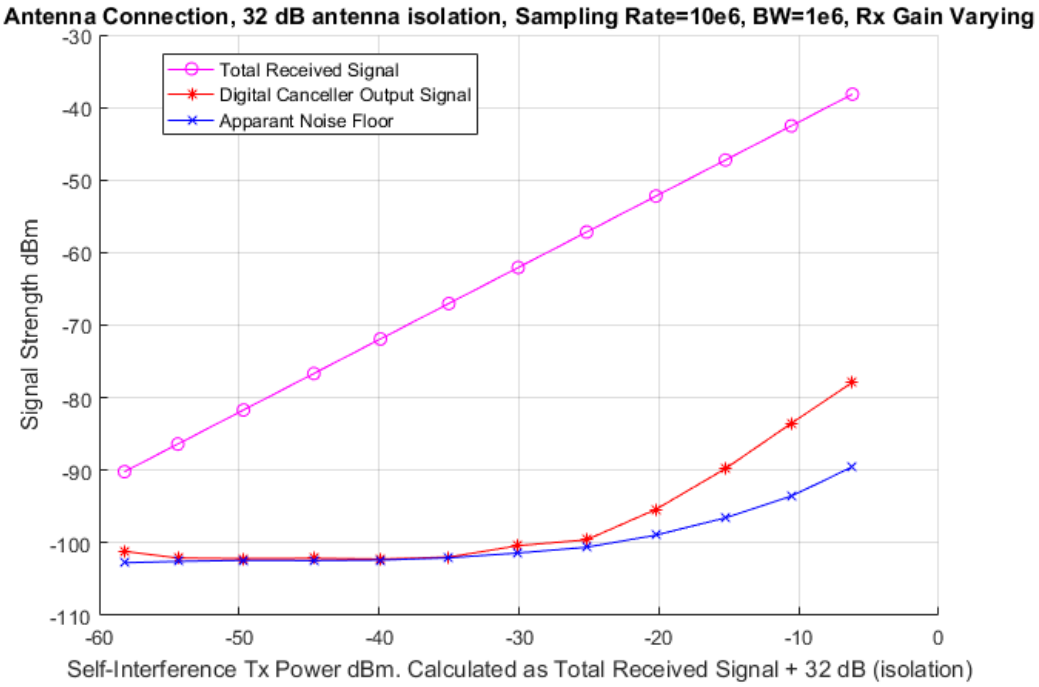

Figure 5.2: Power of the total received signal, residual SI after digital cancellation, and apparent noise floor versus the transmit power of SI. At high powers, there is some residual SI left above noise floor.

The effect of assumed highest nonlinearity order is examined in Figure 5.4. It is evident from this figure that the contribution of the nonlinearity to the self-interference is very minor. Adding the 3rd order nonlinearity to the channel estimation, only 2 dB gain is achieved. Adding another order has made no considerable change. The AD9361 transmitter does not compress (i.e. produce nonlinearities) by design. At the receiver side, the operation is very linear too. The Third-Order Input Intermodulation Intercept Point (IIP3) at the maximum receive path gain is -14 dBm for our carrier frequency. Even at the maximum transmit power case, we receive around $-6dBm - 32dB = -38dBm$ power, for which, obviously, we only use a small portion of receive path gain, which yields an IIP3 of -3 dBm. The difference between the received power and operational IIP3 of our receive path assures us an almost-linear operation.

To clearly see the limit of the self-interference cancellation and the relation between the bandwidth and the cancellation, we used 1, 2, and 3 MHz bandwidth signals and compared their cancellation performances. The results are presented in Fig-

ure 5.5. The maximum achievable cancellation, that is the difference between the total received signal and the apparent noise floor, is drawn in dashed lines. The actual achieved cancellations are drawn with solid lines. Increasing the bandwidth decreases the amount of self-interference cancellation achieved. The most important thing obvious from this figure is the limit to the self-interference cancellation at a certain point, which is for 1 MHz around 42 dB. As is evident from above, the nonlinearity could not be the source for this limit. Importing the parameters of the AD9361 to the simulation environment, the source of this limitation is found to be the phase noise of the local oscillators, as explained in the following section.

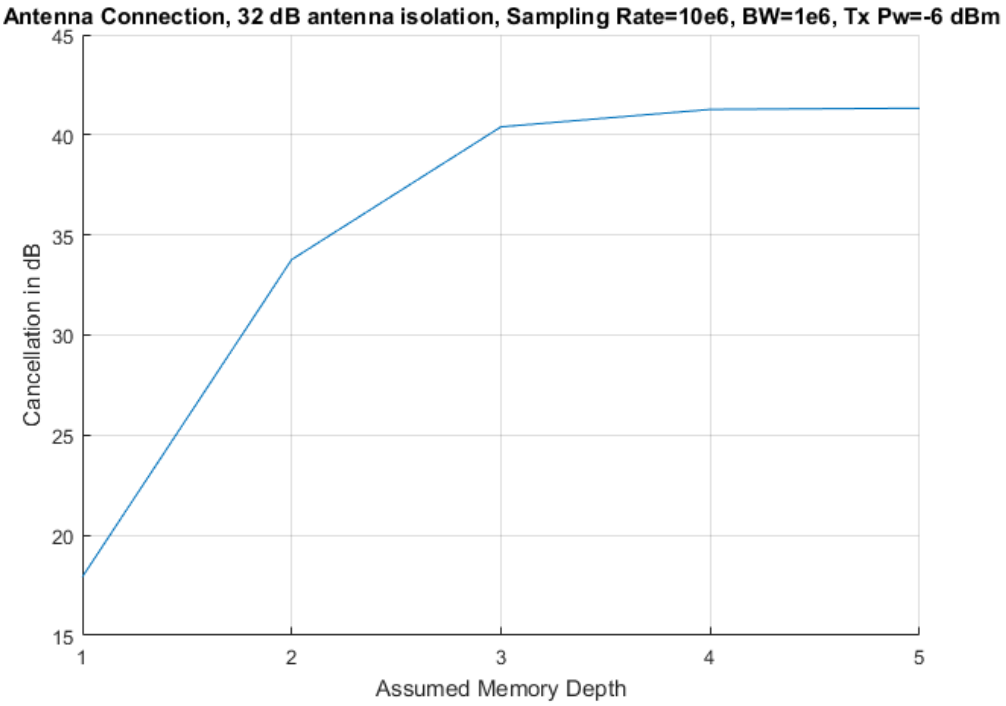

Figure 5.3: The effect of the assumed memory depth of the channel estimation model on cancellation of SI. After 3 taps, there is no considerable change in cancellation.

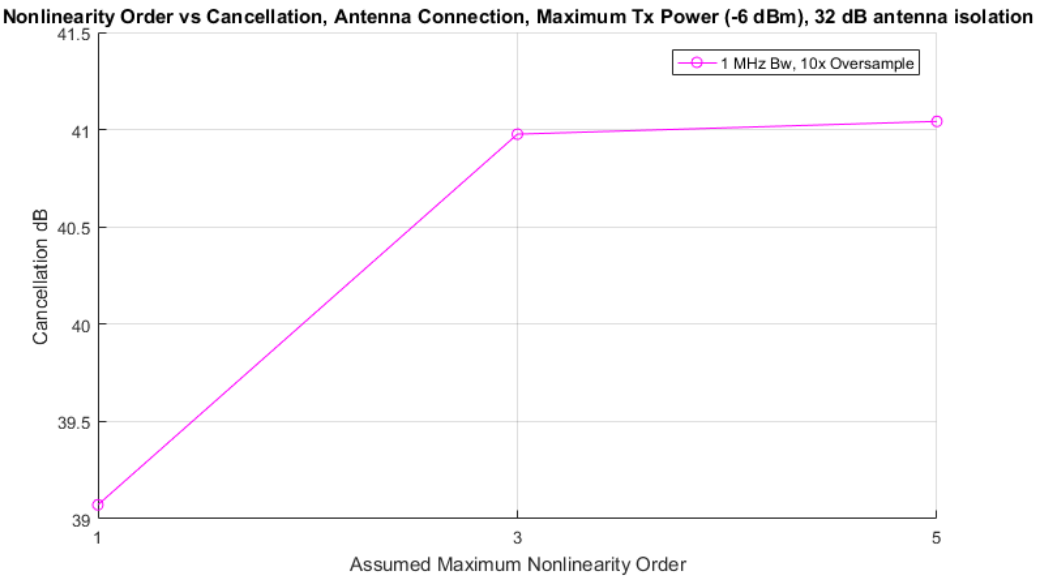

Figure 5.4: The effect of the assumed maximum nonlinearity order of the channel estimation model on cancellation of SI. The transceiver, even at maximum power, operates in a very linear region.

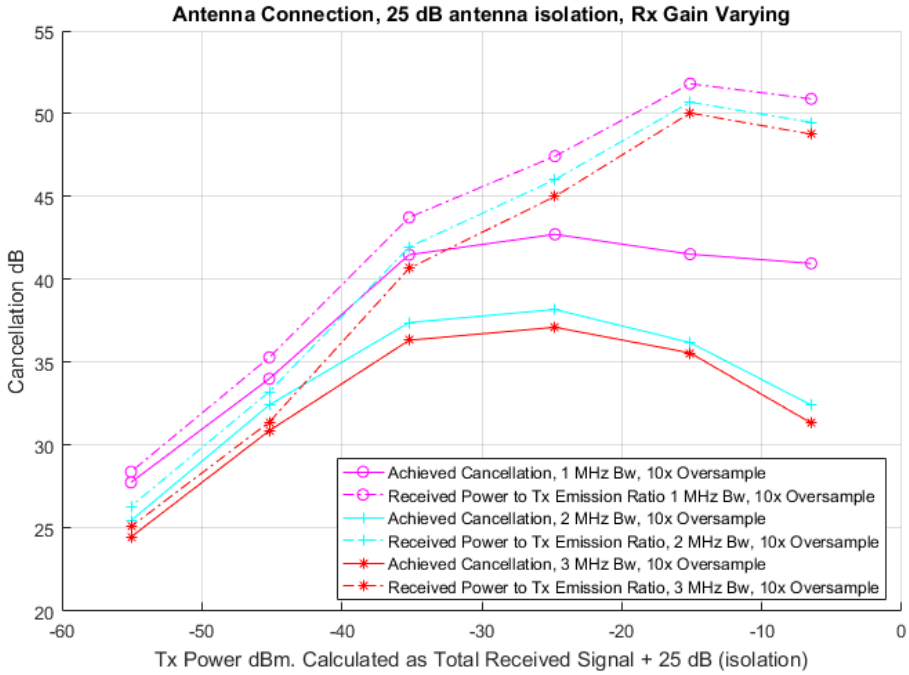

Figure 5.5: Cancellation performance of signals with different bandwidths. Dashed lines show the maximum achievable cancellation, as calculated by total received power to noise floor. Solid lines are the actual performed cancellation.

5.3 Simulation Analysis of Experiment Results

In this section, the simulation environment parameters are imported from the AD9361 data sheet in order to explore further the possible limiting factors of self-interference cancellation. In addition to the RF imperfections presented in Section 4.2.1, which were the power amplifier nonlinearities and IQ-mixer imbalances, phase noise is added on top. Phase noise information used here is retrieved from the AD9361 manual, which were the results of their measurements. Digital cancellation performance under three different scenarios are investigated: no phase noise, shared LO and independent LOs. A random phase noise process is created per the data from AD9361 manual, and for the shared LO case, the same random phase noise is added to the signal in the upconversion and subtracted from it in the downconversion. In the independent LOs case, we created two independent phase noise random processes, each added and subtracted in the relevant places. The effect of limited dynamic range of ADC is not present, which is, although less degrading in our case, is another bottleneck.

Figure 5.6 shows the results when there is no delay between the TX and RX, which also affects the cancellation under phase noise. The no phase noise case shows the best performance, almost canceling out the whole self-interference. The shared LO except at the very high powers almost shows the same performance as if no phase noise is present. However, in the independent LOs case the cancellation is limited at around 40 dB, which agrees with our experiment results. The reason the shared and independent LOs cases are different is the fact that because in the shared case the same noise process is added and subtracted in different stages, it is expected to be cancelled out. It happens so almost perfectly in the hypothetical case where there is no delay between the transmitter and the receiver.

Figure 5.7 shows the results when there is one sample delay between the TX and RX. Even a single sample delay, which is 100ns for 10MHz sampling rate, diminishes the effect of using a shared LO.

The behaviour of cancellation under different sampling rates and bandwidths is investigated in Figure 5.8. Local oscillators are made independent. The same behaviour

seen in the experiments is duplicated in the simulations, namely increasing the sampling rate and bandwidth while keeping the oversampling ratio fixed decreases the cancellation achieved.

As investigated in [84, 87, 138], phase noise is the limiting factor in most practical cases, even in shared LO case, where the negative effect is expected to be less. In [138], a phase noise suppression scheme is proposed, however, it does not gain the cancellation much despite its high complexity. In [138], a similar experiment setup had been used with AD9361 but a different evaluation board, and their results and ours match closely.

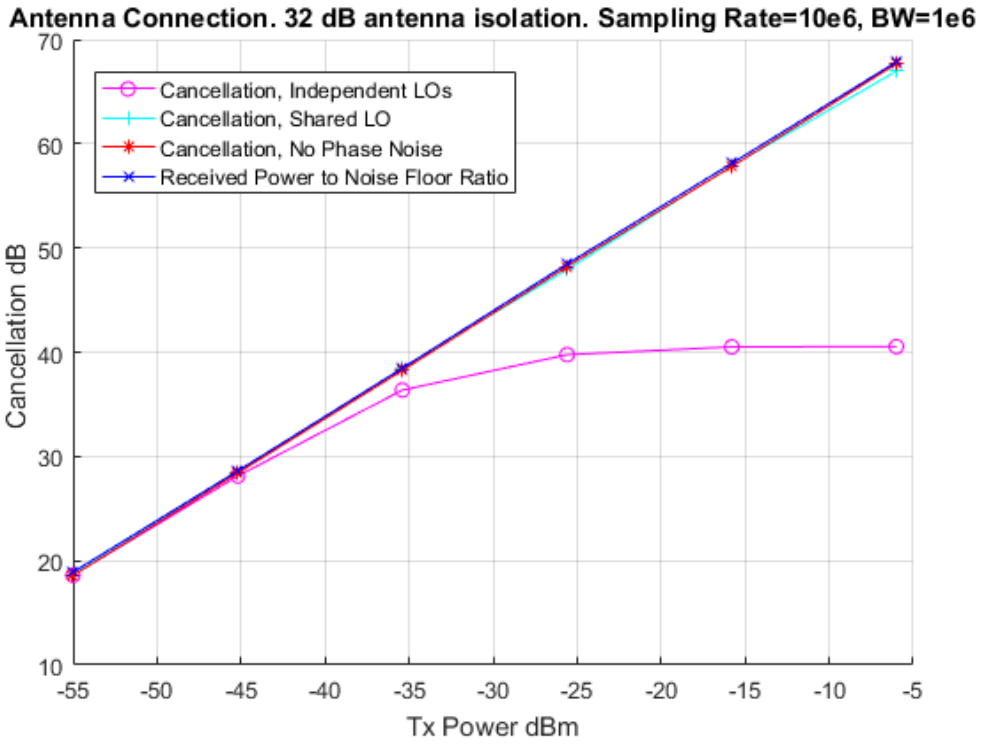

Figure 5.6: Cancellation performances of three different scenarios of phase noise: Independent LOs, a shared LO, and no phase noise at all. The bound for all cases are given as the total received power to the noise floor ratio. Independent LOs case results in a large residual SI in high powers as observed in experiments.

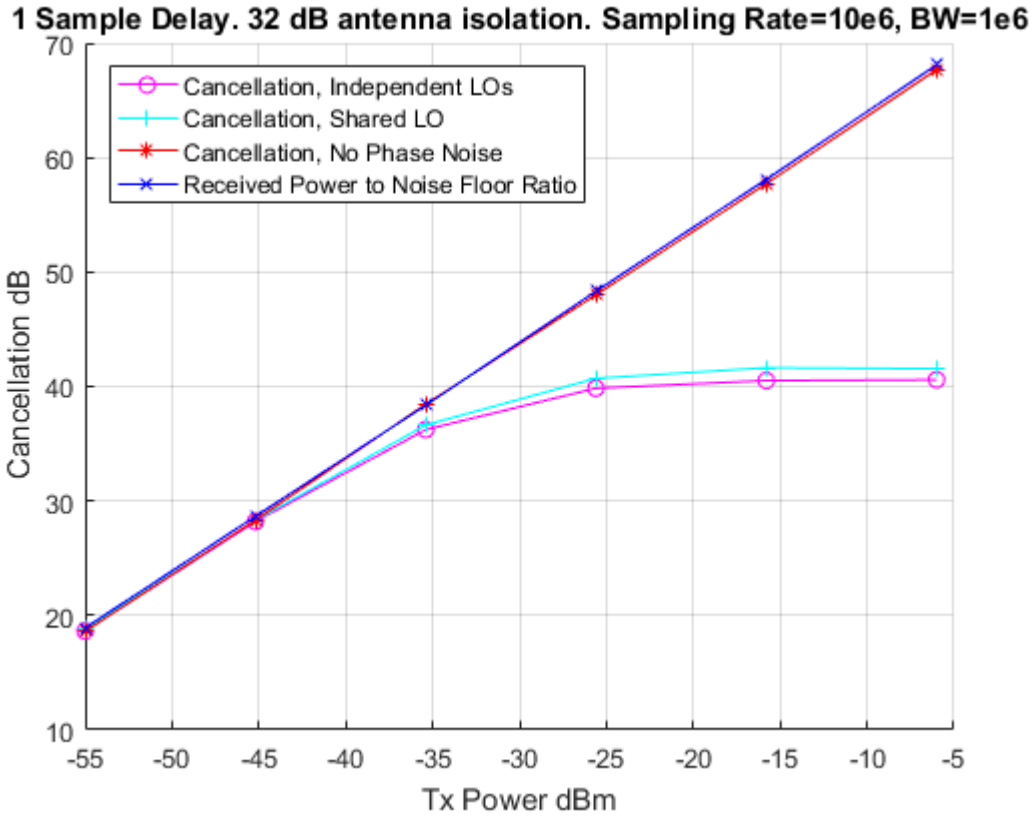

Figure 5.7: Cancellation performances of three different scenarios of phase noise now with one sample delay between Tx and Rx. Shared LO case performs equal with Independent LOs case.

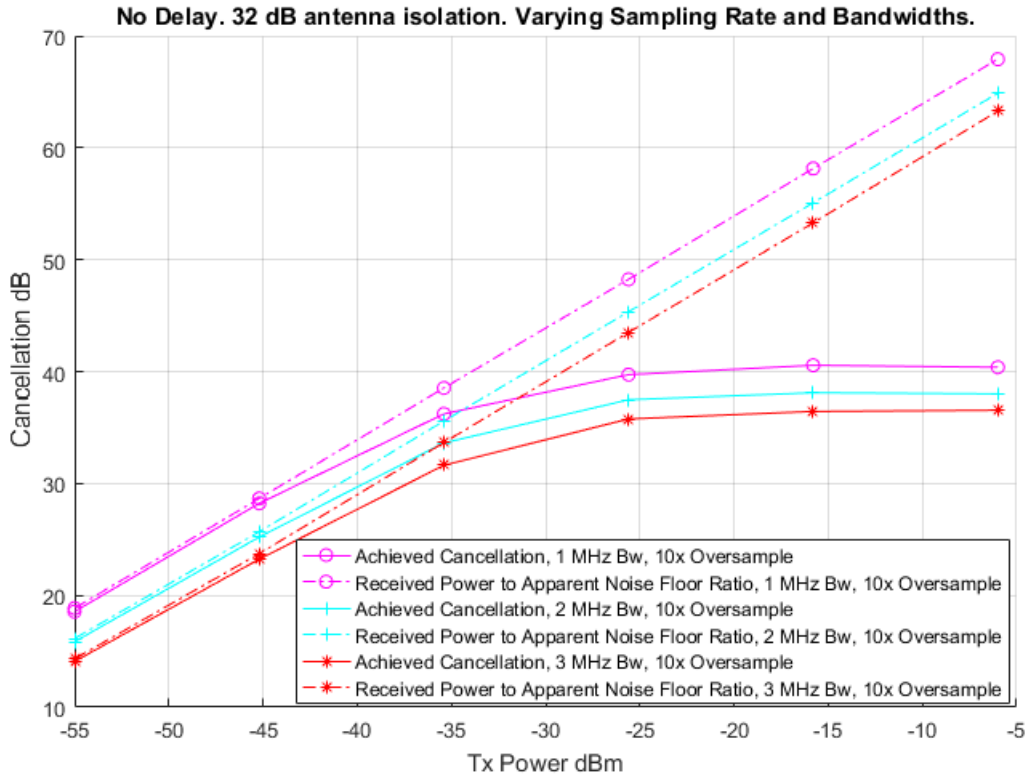

Figure 5.8: Dashed lines are the bounds (total Rx Pwr. to noise floor ratio) and solid lines are the achieved cancellation. The local oscillators are independent. The simulated results here coincide with that of the experiments shown in Figure 5.5.

CHAPTER 6

DISCUSSIONS AND CONCLUSION

6.1 Discussion

Traditional transceivers are not built with in-band full duplex in mind. A strong interferer, self-interference in our case, greatly degrades the performance of the radio link for the signal of interest. For example, in our experiments, in order not to saturate the receive chain with high received power of the self-interference signal, we had to lower the receive path gain to the levels, where noise figure was uncommonly high at around 15 dB. So, although we might cancel out the self-interference so that it does not decrease the signal-to-noise-plus-interference ratio, it will be decreased anyhow because of the increased noise figure. In order to prevent it, the SI signal must be mitigated as much as possible before entering the receive path, by means of propagation and analog domain techniques.

Experiments and simulations demonstrated the bottleneck of in-band full duplex as phase noise. It has been shown experimentally and by simulations, in [84, 87, 138], that even with high complexity phase noise suppression algorithms, it is not possible to cancel its effects completely. One could hope, if not to completely cancel but to diminish its effects, using less noisy local oscillators and sharing the same local oscillator for both transmission and reception where there is not much delay between them.

To the best of our knowledge, there has not been made yet a built-for-the-purpose transceiver for IBFD, although the recent efforts and increasing patents hint in that direction. The IBFD transceiver design should take the bottlenecks shown in the

literature into account, e.g. phase noise, dynamic range, linearity challenges, etc., and focus on overcoming them. Surely, as has been done in the literature so far, any off-the-shelf radio can be, to some capacity, made into IBFD, but with obvious limitations.

Some recommendations from first hand experience during this thesis work can be summarized as follows, although more complete and detailed analysis can be found in the literature as discussed in Section 2.1.2:

- Phase noise is an obvious bottleneck. The best way to overcome it is using better quality local oscillators in the first place. Using shared local oscillators for transmission and reception, to some extent, diminishes the problem, too.

- Cancelling out as much of the SI signal as possible before it even manifests itself in the receive chain is highly recommended. Any practical good IBFD system in the literature does employ the maximum possible amount of propagation domain SIC possible. Facilitating a large amount of SIC in the propagation domain eases the SI problem very much. First of all, it alleviates much of the linearity and dynamic range challenges at the receiver side. Also, it may enable the designer to skip the otherwise necessary complex analog domain cancellation.

6.2 Conclusion

In this master's thesis, the in-band full duplex radios are studied. Its history, briefly, starting from full duplex radars of 1940s is presented, involving the recent advances in full duplex data communications as a way for improving data rate, network performance, secrecy and many other communication aspects.

To fully leverage IBFD, a good self-interference solution must be found. Self interference cancellation in different domains, viz., propagation, analog, and digital, are studied. Among the vast propositions in the literature, a few selected methods are critically presented in detail, their results are verified with our own simulations and experiments, comments on them are made, and some extensions on them are derived.

The results show that the IBFD could be practically implemented.

Experiment and simulation results show the bottleneck of the IBFD as the phase noise of local oscillators. The SIC was fixed at a level that is not enough to leverage IBFD at high transmit powers using only digital SIC and a moderate propagation domain SIC. The indications of experiments were verified with simulations.

Our contributions to the previous literature can be listed as follows:

- The dynamic LMS SIC algorithm, described in Section 3.2.2.1, proposed in [136], had not been tested under dynamic channel conditions. We tested it by simulations under dynamic channel conditions and found the results satisfactory, as described in Section 4.2.2
- The aforementioned dynamic LMS SIC algorithm is extended, exclusively in this thesis, to NLMS and RLS algorithms in Sections 3.2.2.2 and 3.2.2.3, respectively. We tested all dynamic SIC algotithms by simulations under dynamic channel conditions and found their results satisfactory, as described in Section 4.2.2
- For adaptive SIC, it has been proposed in this thesis that, the steady-state error minimization should be favoured over rapid convergence. In fact, the minimum disturbance principle should be followed. Rapidly converging algorithms do tend to manifest fast variations in the signal that will alter the decoding of the intended received signal. Although, this principle is known already, it has not been proposed explicitly for full duplex operation in this context, as far as we know.
- Although, there are already successful full duplex experiments with off-the-shelf or laboratory equipments, the particular experiment setup (i.e., AD-FMCOMMS3-EBZ with AD9361 transceiver) we used is unique. There is an experiment, however, described in [138], that uses AD9361 transceiver with another evaluation board.

Our results and theirs match closely. They also verified their experiment results with simulations, as we did.

REFERENCES

[1] G. Wunder et al., "5GNOW: Non-orthogonal, asynchronous waveforms for future mobile applications," IEEE Commun. Mag., vol. 52, no. 2, pp. 97–105, Feb. 2014.

[2] A. Gohil, H. Modi, and S. K. Patel, "5G technology of mobile communication: A survey," in Proc. ISSP, 2013, pp. 288–292.

[3] G. Wunder et al., "5GNOW: Challenging the LTE design paradigms of orthogonality and synchronicity," in Proc. IEEE 77th Veh. Technol. Conf., 2013, pp. 1–5.

[4] C.-X. Wang et al., "Cellular architecture and key technologies for 5G wireless communication networks," IEEE Commun. Mag., vol. 52, no. 2, pp. 122–130, Feb. 2014.

[5] K. Mallinson, The 2020 Vision for LTE. [Online]. Available: http://www.fiercewireless.com/europe/story/mallinson-2020-vision-lte/ 2012-06-20ixzz1yVRoLFcK

[6] G. Zheng, I. Krikidis, J. Li, A. P. Petropulu, and B. Ottersten, "Improving physical layer secrecy using full-duplex jamming receivers," IEEE Trans. Signal Process., vol. 61, no. 20, pp. 4962–4974, Oct. 2013.

[7] S. Vishwakarma and A. Chockalingam, Sum Secrecy Rate in Full- Duplex Wiretap Channel With Imperfect CSI, arXiv preprint, 2013. [Online]. Available: http://arxiv.org/abs/1311.3918

[8] O. Cepheli, S. Tedik, and G. Kurt, "A high data rate wireless communication system with improved secrecy: Full duplex beamforming," IEEE Commun. Lett., vol. 18, no. 6, pp. 1075–1078, Jun. 2014.

[9] H. Ju, E. Oh, and D. Hong, "Catching resource-devouring worms in nextgeneration wireless relay systems: Two-way relay and full-duplex relay," IEEE Commun. Mag., vol. 47, no. 9, pp. 58–65, Sep. 2009.

[10] H. Ju, S. Lim, D. Kim, H. V. Poor, and D. Hong, "Full duplexity in beamforming-based multi-hop relay networks," IEEE J. Sel. Areas Commun., vol. 30, no. 8, pp. 1554–1565, Sep. 2012.

[11] T. Riihonen, S. Werner, and R. Wichman, "Hybrid full-duplex/halfduplex relaying with transmit power adaptation," IEEE Trans. Wireless Commun., vol. 10, no. 9, pp. 3074–3085, Sep. 2011.

[12] T. Riihonen, S. Werner, and R. Wichman, "Transmit power optimization for multiantenna decode-and-forward relays with loopback selfinterference from full-duplex operation," in Proc. 45th Asilomar Conf. Signals, Syst. Comput., 2011, pp. 1408–1412.

[13] X. Rui, J. Hou, and L. Zhou, "On the performance of full-duplex relaying with relay selection," Electron. Lett., vol. 46, no. 25, pp. 1674–1676, Dec. 2010.

[14] I. Krikidis, H. A. Suraweera, P. J. Smith, and C. Yuen, "Full-duplex relay selection for amplify-and-forward cooperative networks," IEEE Trans. Wireless Commun., vol. 11, no. 12, pp. 4381–4393, Dec. 2012.

[15] M. Jain et al., "Practical, real-time, full duplex wireless," in Proc. 17th Annu. Int. Conf. Mobile Comput. Netw., 2011, pp. 301–312.

[16] Femto Forum, "Interference Management in UMTS Femtocells," February 2010.

[17] Analog Devices, "AD9361." http://www.analog.com.

[18] R. H. Walden, "Analog-to-digital converter survey and analysis," IEEE Journal on Selected Areas in Communications, vol. 17, no. 4, pp. 539–550, 1999.

[19] P. Angeletti, G. Gallinaro, L. Hili, and X. Maufroid, "Evolution of analog to digital conversion technology for wideband space applications," in Proceedings of the 23rd AIAA International Communications Satellite Systems Conference (ICSSC 2005), Rome, Italy, pp. 25–28, 2005.

[20] A. G. Stove, "Linear FMCW radar techniques," IEE Proceedings F (Radar and Signal Processing), vol. 139, no. 5, pp. 343–350, 1992.

[21] F. O'Hara and G. Moore, "A high performance CW receiver using feedthru nulling," Microwave Journal, p. 63, September 1963.

[22] P. Beasley, A. Stove, B. Reits, and B. As, "Solving the problems of a single antenna frequency modulated CW radar," in IEEE International Radar Conference, 1990.

[23] P. Beasley and A. Stove, "Pilot–an example of advanced FMCW techniques," in IEE Colloquium on High Time-Bandwidth Product Waveforms in Radar and Sonar, pp. 10/1–10/5, 1991.

[24] J. G. Kim, S. Ko, S. Jeon, J. W. Park, and S. Hong, "Balanced topology to cancel Tx leakage in CW radar," IEEE Microwave and Wireless Components Letters, vol. 14, Sept. 2004.

[25] W.-K. Kim, M.-Q. Lee, J.-H. Kim, H.-s. Lim, J.-W. Yu, B.-J. Jang, and J.-S. Park, "A passive circulator for RFID application with high isolation using a directional coupler," in 36th European Microwave Conference, pp. 196–199, IEEE, 2006.

[26] C.-Y. Kim, J.-G. Kim, and S. Hong, "A quadrature radar topology with TX leakage canceller for 24-GHz radar applications," IEEE Transactions on Microwave Theory and Techniques, vol. 55, no. 7, pp. 1438–1444, 2007.

[27] K. Lin, Y. E. Wang, C.-K. Pao, and Y.-C. Shih, "A Ka-Band FMCW radar front-end with adaptive leakage cancellation," IEEE Transactions on Microwave Theory and Techniques, vol. 54, no. 12, pp. 4041–4048, 2006.

[28] J.-W. Jung, H.-H. Roh, J.-C. Kim, H.-G. Kwak, M. S. Jeong, and J.-S. Park, "TX leakage Cancellation via a micro controller and high TX-to-RX ssolations covering an UHF RFID frequency band of 908 to 914 MHz," IEEE Microwave and Wireless Components Letters, vol. 18, no. 10, pp. 710–712, 2008.

[29] P. Pursula, M. Kiviranta, and H. Seppa, "UHF RFID reader with reflected power canceller," IEEE Microwave and Wireless Components Letters, vol. 19, no. 1, pp. 48–50, 2009.

[30] K. Lin, R. Messerian, and Y. Wang, "A digital leakage cancellation scheme for monostatic FMCW radar," in Microwave Symposium Digest, 2004 IEEE MTT-S International, vol. 2, pp. 747–750 Vol.2, 2004.

[31] C. Anderson, S. Krishnamoorthy, C. Ranson, T. Lemon, W. Newhall, T. Kummetz, and J. Reed, "Antenna isolation, wideband multipath propagation measurements, and interference mitigation for on-frequency repeaters," in Proceedings of IEEE SoutheastCon, pp. 110 – 114, Mar 2004.

[32] R. Isberg and W. Lee, "Performance tests of a low power cellular enhancer in a parking garage," in IEEE 39th Vehicular Technology Conference, pp. 542–546, IEEE, 1989.

[33] W. T. Slingsby and J. P. McGeehan, "A high-gain cell enhancer," in IEEE 42nd Vehicular Technology Conference, pp. 756–758 vol.2, 1992.

[34] W. Slingsby and J. McGeehan, "Antenna isolation measurements for on-frequency radio repeaters," in Ninth International Conference on (Conf. Publ. No. 407) Antennas and Propagation, pp. 239 –243 vol.1, Apr 1995.

[35] H. Suzuki, K. Itoh, Y. Ebine, and M. Sato, "A booster configuration with adaptive reduction of transmitter-receiver antenna coupling for pager systems," in IEEE Vehicular Technology Conference, Fall 1999, vol. 3, pp. 1516 –1520 vol.3, 1999.

[36] H. Hamazumi, K. Imamura, N. Iai, K. Shibuya, and M. Sasaki, "A study of a loop interference canceller for the relay stations in an SFN for digital terrestrial broadcasting," in IEEE Global Telecommunications Conference, vol. 1, pp. 167–171, 2000.

[37] J. Ma, G. Li, J. Zhang, T. Kuze, and H. Iura, "A new coupling channel estimator for cross-talk cancellation at wireless relay stations," in IEEE Global Telecommunications Conference, pp. 1–6, 2009.

[38] S. J. Kim, J. Y. Lee, J. C. Lee, J. H. Kim, B. Lee, and N. Y. Kim, "Adaptive feedback interference cancellation system (AF-ICS)," in IEEE MTT-S International Microwave Symposium Digest, vol. 1, pp. 627–630 vol.1, 2003.

[39] T. Riihonen, R. Wichman, and J. Hamalainen, "Co-phasing full-duplex relay link with non-ideal feedback information," in IEEE International Symposium on Wireless Communication Systems, pp. 263 –267, Oct. 2008.

[40] T. Riihonen, S. Werner, J. Cousseau, and R. Wichman, "Design of co-phasing allpass filters for full-duplex OFDM relays," in Proceedings of Asilomar Conference on Signals, Systems and Computers, pp. 1030 –1034, Oct. 2008.

[41] D. W. Bliss, P. A. Parker, and A. R. Margetts, "Simultaneous transmission and reception for improved wireless network performance," Conference Proceedings of the IEEE Statistical Signal Processing Workshop, Aug. 2007.

[42] J. Sangiamwong, T. Asai, J. Hagiwara, Y. Okumura, and T. Ohya, "Joint multi-filter design for full-duplex MU-MIMO relaying," in IEEE Vehicular Technology Conference, VTC Spring 2009, pp. 1–5, 2009.

[43] P. Larsson and M. Prytz, "MIMO on-frequency repeater with self-interference cancellation and mitigation," in IEEE 69th Vehicular Technology Conference, VTC Spring 2009, pp. 1–5, 2009.

[44] B. Chun, E.-R. Jeong, J. Joung, Y. Oh, and Y. H. Lee, "Pre-nulling for self-interference suppression in full-duplex relays," in Proceedings: APSIPA ASC 2009: Asia-Pacific Signal and Information Processing Association, 2009 Annual Summit and Conference, pp. 91–97, 2009.

[45] P. Lioliou, M. Viberg, M. Coldrey, and F. Athley, "Self-interference suppression in full-duplex MIMO relays," in Processings of Asilomar Conference on Signals, Systems and Computers, pp. 658–662, 2010.

[46] B. Chun and Y. H. Lee, "A spatial self-interference nullification method for full duplex amplify-and-forward MIMO relays," in Wireless Communications and Networking Conference (WCNC), 2010 IEEE, pp. 1 –6, Apr. 2010.

[47] T. Riihonen, S. Werner, and R. Wichman, "Mitigation of loopback self-interference in full-duplex MIMO relays," IEEE Transactions on Signal Processing, vol. 59, pp. 5983 –5993, Dec. 2011.

[48] T. Riihonen, A. Balakrishnan, K. Haneda, S. Wyne, S. Werner, and R. Wichman, "Optimal eigenbeamforming for suppressing selfinterference in full-duplex MIMO relays," in 45th Annual Conference on Information Sciences and Systems (CISS), pp. 1–6, IEEE, 2011.

[49] B. Day, A. Margetts, D. Bliss, and P. Schniter, "Full-duplex MIMO relaying: Achievable rates under limited dynamic range," IEEE Journal on Selected Areas in Communications, vol. 30, pp. 1541 –1553, September 2012.

[50] H. Ju, E. Oh, and D. Hong, "Improving efficiency resource usage in two-hop full duplex relay systems based on resource sharing and interference cancellation," IEEE Transactions on Wireless Communications, vol. 8, Aug. 2009.

[51] O. Somekh, O. Simeone, H. Poor, and S. Shamai, "Cellular systems with full-duplex amplify-and-forward relaying and cooperative base-stations," in IEEE International Symposium on Information Theory, pp. 16–20, 2007.

[52] S. Sohaib and D. K. C. So, "Asynchronous polarized cooperative mimo communication," in Proceedings of Vehicular Technology Conference, pp. 1–5, April 2009.

[53] H. Ju, E. Oh, and D. Hong, "Catching resource-devouring worms in next-generation wireless relay systems: Two-way relay and full-duplex relay," IEEE Communications Magazine, vol. 47, pp. 58 –65, September 2009.

[54] V. Cadambe and S. Jafar, "Can feedback, cooperation, relays and full duplex operation increase the degrees of freedom of wireless networks?," in IEEE International Symposium on Information Theory (ISIT), pp. 1263 –1267, Jul. 2008.

[55] S. Simoens, O. Munoz-Medina, J. Vidal, and A. del Coso, "On the Gaussian MIMO relay channel with full channel state information," IEEE Transactions on Signal Processing, pp. 3588–3599, Sept. 2009.

[56] T. Riihonen, S. Werner, R. Wichman, and E. Zacarias, "On the feasibility of full-duplex relaying in the presence of loop interference," in Proceedings of IEEE workshop on Signal Processing and Advances in Wireless Communications, 2009.

[57] T. Riihonen, K. Haneda, S. Werner, and R. Wichman, "SINR analysis of full-duplex OFDM Repeaters," in PIMRC, Sept. 2009.

[58] K. Yamamoto, K. Haneda, H. Murata, and S. Yoshida, "Optimal Transmission Scheduling for a hybrid of full- and half-duplex Relaying," IEEE Communications Letters, vol. 15, no. 3, pp. 305–307, 2011.

[59] Y. K. Song and D. Kim, "Convergence of distributed power control with full-duplex amplify-and-forward relays," in International Conference on Wireless Communications Signal Processing, pp. 1–5, 2009.

[60] Y. Y. Kang and J. H. Cho, "Capacity of MIMO wireless channel with full-duplex amplify-and-forward relay," in IEEE 20th International Symposium on Personal, Indoor and Mobile Radio Communications, pp. 117–121, 2009.

[61] T. Baranwal, D. Michalopoulos, and R. Schober, "Outage analysis of multihop full duplex relaying," IEEE Communications Letters, vol. 17, no. 1, pp. 63–66, 2013.

[62] D. W. Bliss and S. Govindasamy, Adaptive Wireless Communications: MIMO Channels and Networks. Cambridge University Press, 2013.

[63] S. Chen, M. A. Beach, and J. P. McGeehan, "Division-free duplex for wireless applications," in IEEE Electronics Letters, vol. 34, 1998.

[64] M. Duarte and A. Sabharwal, "Full-duplex wireless communications using off-the-shelf radios: Feasibility and first results," in Proceedings of Asilomar Conference on Signals, Systems and Computers, 2010.

[65] J. I. Choi, M. Jain, K. Srinivasan, P. Levis, and S. Katti, "Achieving single channel, full duplex wireless communications," in Proceedings of ACM Mobicom, 2010.

[66] M. A. Khojastepour, K. Sundaresan, S. Rangarajan, X. Zhang, and S. Barghi, "The case for antenna cancellation for scalable full-duplex wireless communications," in Proceedings of the 10th ACM Workshop on HotNets, 2011.

[67] M. Jain, J. I. Choi, T. Kim, D. Bharadia, K. Srinivasan, S. Seth, P. Levis, S. Katti, and P. Sinha, "Practical, real-time, full duplex wireless," in Proceedings of the ACM Mobicom, Sept. 2011.

[68] A. K. Khandani, "Shaping the future of wireless: Two-way connectivity." http://www.nortel-institute.uwaterloo.ca/content/Shaping Future of Wireless Two-way Connectivity 18ne2012.pdf, 2015.

[69] A. Sahai, G. Patel, and A. Sabharwal, "Pushing the limits of full-duplex: Design and real-time implementation, http://arxiv.org/abs/1107.0607," in Rice University Technical Report TREE1104, 2015.

[70] B. Radunovic, D. Gunawardena, P. Key, A. P. N. Singh, V. Balan, and G. Dejean, "Rethinking indoor wireless: Low power, low frequency, full duplex," tech. rep., Microsoft Research, 2009.

[71] M. Duarte, C. Dick, and A. Sabharwal, "Experiment-driven characterization of full-duplex wireless systems," IEEE Transactions on Wireless Communications, vol. 11, no. 12, pp. 4296–4307, 2012.

[72] E. Aryafar, M. Khojastepour, K. Sundaresan, S. Rangarajan, and M. Chiang, "MIDU: Enabling MIMO full duplex," in Proceedings of ACM MobiCom, 2012.

[73] M. Duarte, A. Sabharwal, V. Aggarwal, R. Jana, K. Ramakrishnan, C. Rice, and N. Shankaranarayanan, "Design and characterization of a full-duplex multi-antenna system for WiFi networks," to appear in IEEE Transactions on Vehicular Communications, (arXiv preprint arXiv:1210.1639), 2013.

[74] M. Duarte, Full-duplex Wireless: Design, Implementation and Characterization. PhD thesis, Rice University, April 2012.

[75] E. Everett, M. Duarte, C. Dick, and A. Sabharwal, "Empowering full-duplex wireless communication by exploiting directional diversity," in Proceedings of Asilomar Conference on Signals, Systems and Computers, IEEE, 2011.

[76] E. Everett, A. Sahai, and A. Sabharwal, "Passive self-interference suppression for full-duplex infrastructure nodes." IEEE Transactions on Wireless Communications, to be published. arXiv preprint arXiv:1302.2185.

[77] E. Everett, "Full-duplex infrastructure nodes: Achieving long range with half-duplex mobiles," Master's thesis, Rice University, 2012.

[78] M. E. Knox, "Single antenna full duplex communications using a common carrier," in IEEE 13th Annual Wireless and Microwave Technology Conference (WAMICON), pp. 1–6, 2012.

[79] D. Bharadia, E. McMilin, and S. Katti, "Full duplex radios," in Proceedings of ACM SIGCOMM, 2013.

[80] A. K. Khandani, "Methods for spatial multiplexing of wireless two-way channels," Oct. 2010. US Patent 7,817,641.

[81] L. W. Fullerton, "Full duplex ultrawide-band communication system and method," 1997. US Patent 5,687,169.

[82] S. N. Stitzer, "Full duplex communication system apparatus using frequency selective limiters," 1982. US Patent 4,325,140.

[83] A. Sahai, G. Patel, C. Dick, and A. Sabharwal, "Understanding the impact of phase noise on active cancellation in wireless full-duplex," in Proceedings of Asilomar Conference on Signals, Systems and Computers, 2012.

[84] A. Sahai, G. Patel, C. Dick, and A. Sabharwal, "On the impact of phase noise on active cancellation in wireless full-duplex," arXiv preprint arXiv:1212.5462, 2012.

[85] D. W. Bliss, T. M. Hancock, and P. Schniter, "Hardware phenomenological effects on cochannel full-duplex MIMO relay performance," IEEE Asilomar Conference on Signals, Systems and Computers, 2012.

[86] E. Ahmed, A. Eltawil, and A. Sabharwal, “Rate gain region and design tradeoffs for full-duplex wireless communications,” submitted to IEEE Transactions on Wireless Communications, 2013.

[87] Syrjala, V.; Valkama, M.; Anttila, L.; Riihonen, T.; Korpi, D., "Analysis of Oscillator Phase-Noise Effects on Self-Interference Cancellation in Full-Duplex OFDM Radio Transceivers," in Wireless Communications, IEEE Transactions on , vol.13, no.6, pp.2977-2990, June 2014

[88] D. Korpi, T. Riihonen, V. Syrjala, L. Anttila, M. Valkama, and R. Wichman, “Full-duplex transceiver system calculations: Analysis of ADC and linearity challenges,” arXiv preprint arXiv:1401.3538, 2014.

[89] B. Day, A. Margetts, D. Bliss, and P. Schniter, “Full-duplex bidirectional MIMO: Achievable rates under limited dynamic range,” IEEE Transactions on Signal Processing, vol. 60, pp. 3702 –3713, July 2012.

[90] D. Korpi, S. Venkatasubramanian, T. Riihonen, L. Anttila, S. Otewa, C. Icheln, K. Haneda, S. Tretyakov, M. Valkama, and R. Wichman, “Advanced Self-Interference Cancellation and Multi-Antenna Solutions for Full-Duplex Radios,” in Proceedings of Asilomar Conference on Signals, Systems and Computers, 2013.

[91] L. Anttila, D. Korpi, and V. Syrjala, “Cancellation of Power Amplifier Induced Nonlinear Self-Interference in Full-Duplex Transceivers,” in Proceedings of Forty Seventh Asilomar Conference on Signals, Systems and Computers, 2013.

[92] Y.-S. Choi and H. Shirani-Mehr, “Simultaneous transmission and reception: Algorithm, design and system level performance,” Wireless Communications, IEEE Transactions on, vol. 12, pp. 5992–6010, December 2013.

[93] H. Holma and A. Toskala, eds., WCDMA for UMTS: Radio Access for Third Generation Mobile Communications. Wiley, 3rd ed., 2004.

[94] A. Kiayani, L. Anttila, and M. Valkama, “Digital Suppression of Power Amplifier Spurious Emissions at Receiver Band in FDD Transceivers,” Signal Processing Letters, IEEE, vol. 21, pp. 69–73, Jan 2014.

[95] M. Omer, R. Rimini, P. Heidmann, and J. Kenney, “A compensation scheme to allow full duplex operation in the presence of highly nonlinear microwave components for 4G systems,” in Microwave Symposium Digest (MTT), 2011 IEEE MTT-S International, pp. 1–4, June 2011.

[96] A. Frotzscher and G. Fettweis, “Digital compensation of transmitter leakage in FDD zero-IF receivers,” Transactions on Emerging Telecommunications Technologies, vol. 23, no. 2, pp. 105–120, 2012.

[97] A. Kiayani, L. Anttila, and M. Valkama, "Modeling and dynamic cancellation of TX-RX leakage in FDD transceivers," in Circuits and Systems (MWSCAS), 2013 IEEE 56th International Midwest Symposium on, pp. 1089–1094, Aug 2013.

[98] C. S. Vaze and M. K. Varanasi, "The degrees of freedom of MIMO networks with full-duplex receiver cooperation but no CSIT," arXiv preprint arXiv:1209.1291, 2012.

[99] Q. Geng, S. Kannan, and P. Viswanath, "Interactive interference alignment," arXiv preprint arXiv:1211.0985, 2012.

[100] A. Sahai, S. Diggavi, and A. Sabharwal, "On degrees of freedom of full-duplex uplink/downlink channel," in ITW, Sept. 2013.

[101] J. Bai and A. Sabharwal, "Decode-and-cancel for interference cancellation in a three-node full-duplex network," in Proceedings of Asilomar Conference on Signals, Systems and Computers, 2012.

[102] J. Bai and A. Sabharwal, "Distributed full-duplex via wireless side-channels: Bounds and protocols," IEEE Transactions on Wireless Communications, vol. 12, no. 8, pp. 4162–4173, 2013.

[103] W. Cheng, X. Zhang, and H. Zhang, "Full duplex wireless communications for cognitive radio networks," arXiv:1105.0034v1, 2011.

[104] W. Schacherbauer, A. Springer, T. Ostertag, C. Ruppel, and R. Weigel, "A flexible multiband frontend for software radios using high IF and active interference cancellation," in IEEE International Microwave Simpossium, 2001.

[105] A. Raghavan, E. Gebara, E. M. Tentzeris, and J. Laskar, "Analysis and design of an interference canceller for collocated radios," IEEE Transactions on Microwave Theory and Techniques, vol. 53, no. 3498-3508, 2005.

[106] N. Singh, D. Gunawardena, A. Proutiere, B. Radunovic, H. Balan, and P. Key, "Efficient and fair MAC for wireless networks with self-interference cancellation," in International Symposium on Modeling and Optimization in Mobile, Ad Hoc and Wireless Networks (WiOpt), pp. 94 –101, May 2011.

[107] S. Sen, R. Roy Choudhury, and S. Nelakuditi, "No time to countdown: migrating backoff to the frequency domain," in Proceedings of ACM Mobicom, (New York, NY, USA), 2011.

[108] P. Weeraddana, M. Codreanu, M. Latva-aho, and A. Ephremides, "On the effect of self-interference cancelation in multihop wireless networks," EURASIP Journal on Wireless Communications and Networking, vol. 2010, no. 1, p. 513952, 2010.

[109] D. Ramirez and B. Aazhang, "Optimal routing and power allocation for wireless networks with imperfect full-duplex nodes," IEEE Transactions on Wireless Communications, vol. 12, no. 9, pp. 4692–4704, 2013.

[110] X. Fang, D. Yang, and G. Xue, "Distributed algorithms for multipath routing in full-duplex wireless networks," in Proceedings of the 2011 IEEE Eighth International Conference on Mobile Ad-Hoc and Sensor Systems, MASS '11, (Washington, DC, USA), pp. 102–111, IEEE Computer Society, 2011.

[111] W. Mesbah and T. Davidson, "Optimal power allocation for full-duplex cooperative multiple access," in IEEE International Conference on Acoustics, Speech and Signal Processing (ICASSP), vol. 4, pp. IV–IV, 2006.

[112] L. Zhang, J. Luo, and D. Guo, "Neighbour discovery for wireless networks via compressed sensing," Performance Evaluation, vol. 70, pp. 457–471, 2013.

[113] L. Zhang and D. Guo, "Virtual full-duplex wireless broadcasting via compressed sensing," to appear in IEEE/ACM Transactions on Networking, 2014.

[114] M. Gan, D. Guo, and X. Dai, "Distributed ranging and localization for wireless networks via compressed sensing," arXiv preprint arXiv:1308.3548, 2013.

[115] O. Somekh, O. Simeone, H. V. Poor, and S. Shamai, "Cellular systems with full-duplex compress-and-forward relaying and cooperative base stations," in Proc. IEEE Int. Symp. Inf. Theory, 2008, pp. 2086–2090.

[116] O. Somekh, O. Simeone, H. V. Poor, and S. Shamai, "Cellular systems with non-regenerative relaying and cooperative base stations," IEEE Trans. Wireless Commun., vol. 9, no. 8, pp. 2654–2663, Aug. 2010.

[117] I. Akyildiz, W. Lee, M. Vuran, and S. Mohanty. Next generation/dynamic spectrum access/cognitive radio wireless networks: A survey. Computer Networks, 50 (13) 212782159, 2006.

[118] W. Cheng, X. Zhang, and H. Zhang. Full duplex spectrum sensing in nontime-slotted cognitive radio networks. In Military Communications Conference MILCOM, pages 102981034, 2011.

[119] E. Ahmed, A. Eltawil, and A. Sabharwal. Simultaneous transmit and sense for cognitive radios using full-duplex: A first study. In Proc. Antennas and Propagation Society International Symposium (APSURSI), pages 182, 2012.

[120] D. Kim, S. Park, H. Ju, and D. Hong, "Transmission capacity of fullduplex based two-way ad-hoc networks with ARQ protocol," IEEE Trans. Veh. Technol., vol. 63, no. 7, pp. 3167–3183, Sep. 2014.

[121] J. Zhang, L. Fu, and X. Wang. Asymptotic analysis on secrecy capacity in large-scale wireless networks, 2013.

[122] G. Zheng, I. Krikidis, J. Li, A.P. Petropulu, and B. Ottersten. Improving physical layer secrecy using full-duplex jamming receivers. IEEE Transactions on Signal Processing, 61(20):496284974, 2013.

[123] D. Halperin, T. Anderson, and D. Wetherall. Taking the sting out of carrier sense: interference cancellation for wireless LANs. In Proc. 14th ACM international conference on Mobile computing and networking, pages 3398350, New York, NY, USA, 2008. ACM.

[124] T. Snow, C. Fulton, and W. J. Chappell, "Transmit-receive duplexing using digital beamforming system to cancel self-interference," IEEE Transactions on Microwave Theory and Techniques, vol. 59, no. 12, pp. 3494–3503, 2011.

[125] Kaufman, B.; Lilleberg, J.; Aazhang, B., "An analog baseband approach for designing full-duplex radios," in Signals, Systems and Computers, 2013 Asilomar Conference on , vol., no., pp.987-991, 3-6 Nov. 2013

[126] T. Riihonen and R. Wichman, "Analog and digital self-interference cancellation in full-duplex MIMO-OFDM transceivers with limited resolution in A/D conversion," in Proceedings of Asilomar Conference on Signals, Systems and Computers, pp. 45–49, November 2012.

[127] Korpi, D.; Anttila, L.; Syrjala, V.; Valkama, M., "Widely Linear Digital Self-Interference Cancellation in Direct-Conversion Full-Duplex Transceiver," in Selected Areas in Communications, IEEE Journal on , vol.32, no.9, pp.1674-1687, Sept. 2014

[128] E. Ahmed, A. M. Eltawil, and A. Sabharwal, "Self-interference cancellation with nonlinear distortion suppression for full-duplex systems.," CoRR, vol. abs/1307.3796, 2013

[129] Anttila, L.; Korpi, D.; Antonio-Rodriguez, E.; Wichman, R.; Valkama, M., "Modeling and efficient cancellation of nonlinear self-interference in MIMO full-duplex transceivers," in Globecom Workshops (GC Wkshps), 2014 , vol., no., pp.777-783, 8-12 Dec. 2014

[130] Huusari, T.; Yang-Seok Choi; Liikkanen, P.; Korpi, D.; Talwar, S.; Valkama, M., "Wideband Self-Adaptive RF Cancellation Circuit for Full-Duplex Radio: Operating Principle and Measurements," in Vehicular Technology Conference (VTC Spring), 2015 IEEE 81st , vol., no., pp.1-7, 11-14 May 2015

[131] S. Haykin, Adaptive Filter Theory, 4th ed. ed. Englewood Cliffs, NJ, USA: Prentice-Hall, 2001.

[132] L. Ding, G. Zhou, D. Morgan, Z. Ma, J. Kenney, J. Kim, and C. Giardina, "A robust digital baseband predistorter constructed using memory polynomials," IEEE Transactions on Communications, vol. 52, no. 1, pp. 159–165, 2004.

[133] M. Isaksson, D. Wisell, and D. Ronnow, “A comparative analysis of behavioral models for RF power amplifiers,” IEEE Transactions on Microwave Theory and Techniques, vol. 54, no. 1, pp. 348–359, 2006.

[134] L. Anttila, P. Handel, and M. Valkama, “Joint mitigation of power amplifier and I/Q modulator impairments in broadband direct-conversion transmitters,” IEEE Transactions on Microwave Theory and Techniques, vol. 58, no. 4, pp. 730–739, 2010.

[135] H. Ku and J. Kenney, “Behavioral modeling of nonlinear RF power amplifiers considering memory effects,” IEEE Transactions on Microwave Theory and Techniques, vol. 51, no. 12, pp. 2495–2504, 2003.

[136] D. Korpi, Y.-S. Choi, T. Huusari, L. Anttila, S. Talwar, and M. Valkama, "Adaptive nonlinear digital self-interference cancellation for mobile inband full-duplex radio: Algorithms and RF measurements," in Proc. IEEE Global Communications Conference (GLOBECOM), Dec. 2015

[137] “LTE; evolved universal terrestrial radio access (E-UTRA); user equipment (UE) radio transmission and reception (3GPP TS 36.101 version 11.2.0 release 11),” ETSI, Sophia Antipolis Cedex, France.

[138] E. Ahmed and A. M. Eltawil, "On Phase Noise Suppression in Full-Duplex Systems," in IEEE Transactions on Wireless Communications, vol. 14, no. 3, pp. 1237-1251, March 2015. doi: 10.1109/TWC.2014.2365536

[139] IEEE 802.11. http://www.ieee802.org, August 2016

[140] W. Kester, The Data Conversion Handbook, Newnes, 2005.

APPENDIX A

ANALOG DOMAIN SIMULATIONS

In this appendix, the schematics used in simulations in ADS are presented. In Schematic A.1, the whole simulation environment is presented with the weight calculation block encapsulated in a subsystem. In Schematic A.2, the weight calculation subsystem is expanded and shown in whole. All blocks in the schematic are predefined in ADS. Basically the systems runs so: the signal is generated and then run through a nonlinear power amplifier. Then, one branch is tapped for producing the replica of the self-interference signal, and two branches below produce the received self-interference. These last two branches emulate the circulator or a reflected path from antenna. The produced replica is subtracted from the received signal by means of a 180 degree phase shifter and an adder.

In Figure A.2, the weight calculation block is explicitly shown. It does the operation as defined in 3.14. White noise is added at relevant stages to emulate for the noise added by the active components in an actual device. There are also gain imbalances present as shown in the middle.

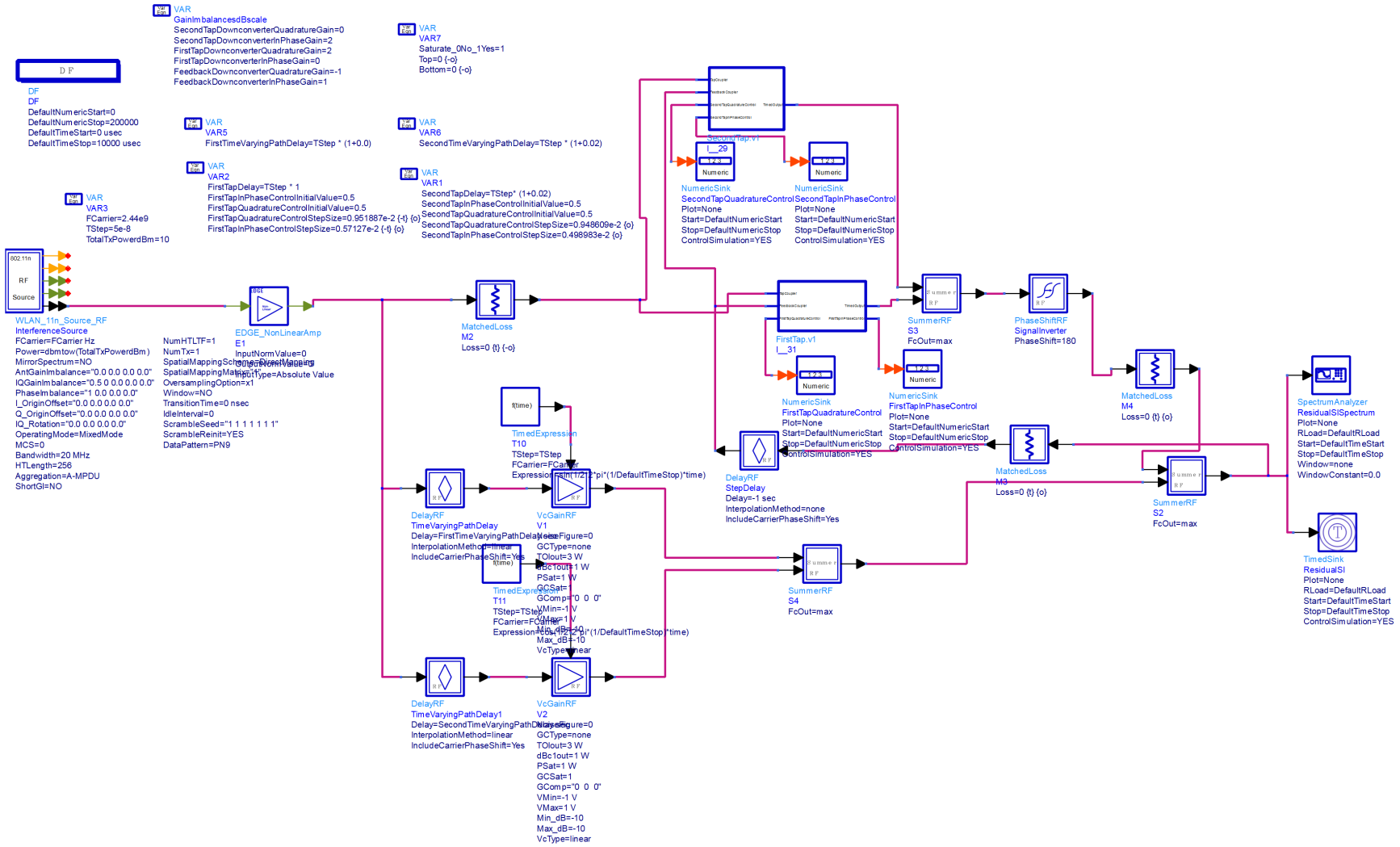

Figure A.1: Simulation Setup in ADS

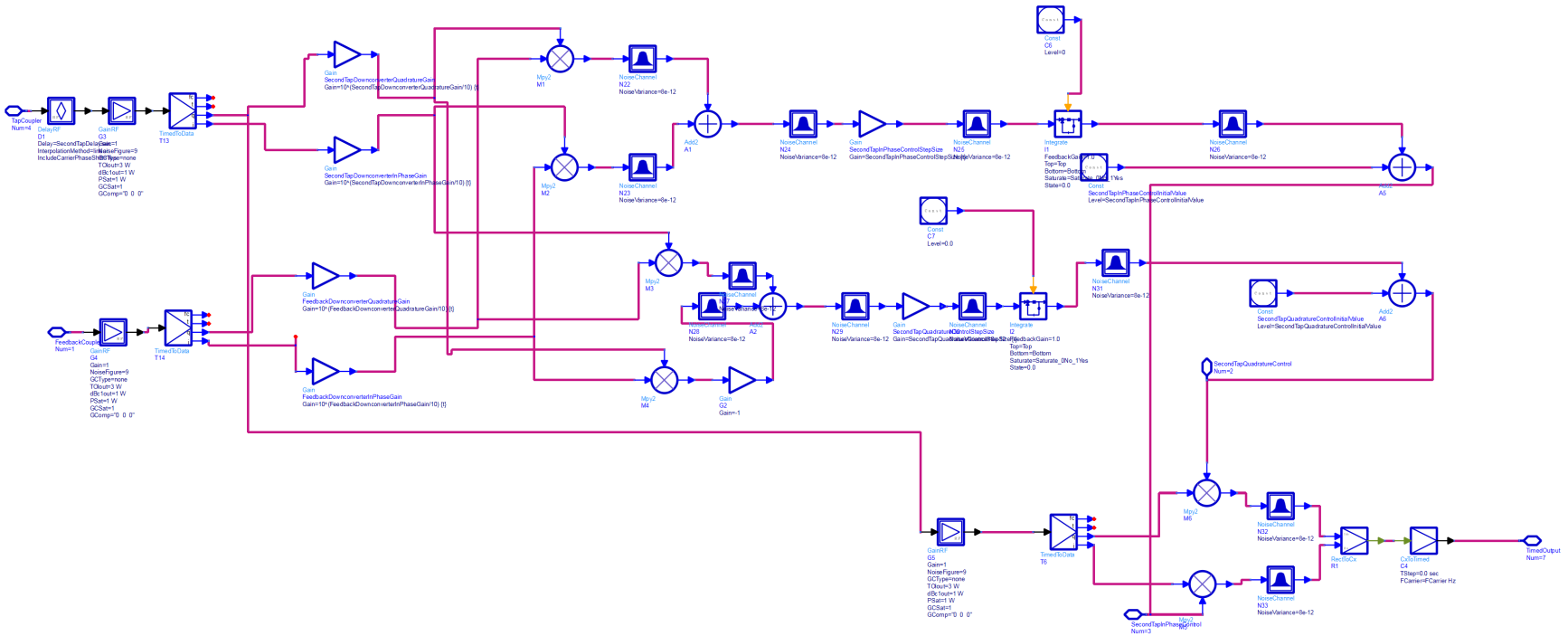

Figure A.2: The weight calculation subsystem of the Schematic A.1 is expanded here.

APPENDIX B

DIGITAL DOMAIN SIMULATIONS

In this appendix, the schematic used in simulations in Matlab/Simulink and a sample Matlab code for digital cancellation are presented. The intended received signal in the schematic is generated in a subsystem and is same as the self-interference signal generation. The parameters for the transmit and receive power amplifiers are calculated by the Simulink's prebuilt General Amplifier model, which can be accessed from the general Help interface of Matlab. The analog cancellation is a predefined block available in Simulink.

```
% Digital Cancellation Sample Code
% x and y are to be imported
% from the Simulink model as shown on the
% schematic. x is the baseband transmit
% self-interference, y is the total
% received signal

%%% Following are the only parameters
% to be determined by the user
P=5; %maximum assumed nonlinearity order
% of the chn. est. model
M=5; %maximum assumed memory depth
% of the chn. est. model
N=length(x); %number of samples to be used
% in chn. est. max is length(x)
```

```
%%% Construction of the bases psi
psi_column_size=sum((1:2:P)+1)*M;
psi_row_size=length(x);
psi=zeros(psi_row_size,psi_column_size);
psiorder=0; % initialisation
for p=1:2:P
for q=0:p
psi(1:psi_row_size,1+(psiorder*M):(psiorder+1)*M)=...
toeplitz((x.^q).*...
(conj(x).^(p-q)),zeros(1,M));
psiorder=psiorder+1;
end
end

%%% Least squares channel estimation
h_estimate=(psi(1:N,1:psi_column_size)'*...
psi(1:N,1:psi_column_size))^-1*...
psi(1:N,1:psi_column_size)'*y(1:N,1);

%%% Producing the replica of SI
r=psi(1:psi_row_size,1:psi_column_size)*h_estimate;

%%% Subtraction of the replica of SI
% from the whole received signal.
% Output is the residual SI or the signal to be sent
% for decoding of intended received signal.
e=y(1:psi_row_size)-r;
```

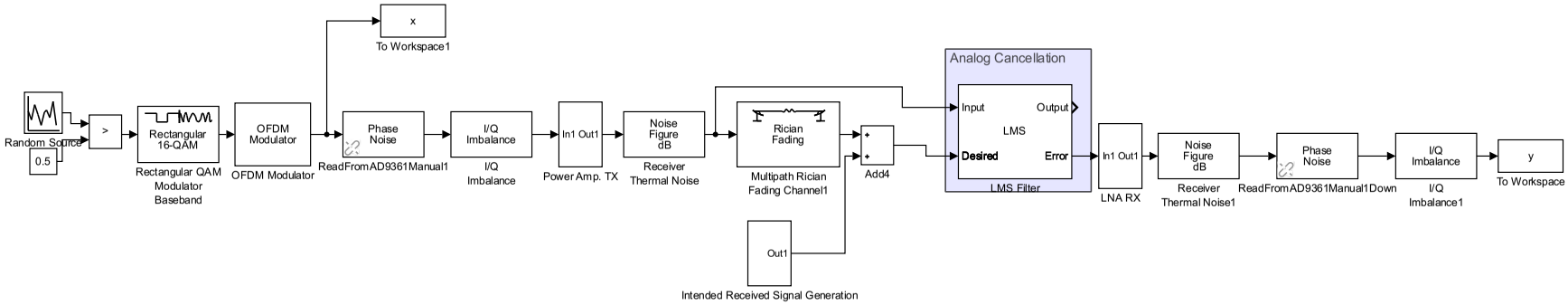

Figure B.1: The signal x is the tapped signal and y is the output that will be fed to the intended received signal decoder.